ÉCOLE POLYTECHNIQUE FÉDÉRALE DE LAUSANNE

Energy Management System for the Train Inspection Monorail

Engineering internship at CERN with master project

Master in Electrical and Electronic Engineering, Smart Grids orientation

12/08/2016

EPFL supervisor: Pr. Mario Paolone

CERN supervisor: Mario Di Castro

Student: Léo Sibut

Academic year 2015/2016

ÉCOLE POLYTECHNIQUE FÉDÉRALE DE LAUSANNE

Acknowledgements

I sincerely would like to thank my EPFL supervisor, Professor Mario Paolone, for accepting to supervise my Master thesis at CERN, for all his wise suggestions but also for having found time to help me during this project despite his busy timetable.

I would also like to thank my CERN supervisor Mario Di Castro for guiding me during the development of this project and for the wise advices he has provided during my stay at CERN.

Last but not least, I would like to express my gratitude to my parents for their support, their encouragements and for believing in me during my years spent at EPFL.

Abstract

This master thesis addresses at the battery energy management of a battery powered vehicle; the Train Inspection Monorail or TIM. This work is an attempt at improving the autonomy of TIM but also at improving the reliability of its operation by using the energy stored in the battery in the smartest possible way.

The main problem encountered with the previously existing solution was the lack of accuracy on the State-Of-Charge (SOC) estimation. In consequences the critical lower SOC limit is set to a relatively high value in order to avoid a break-down of the train in the middle of the tunnel, away from a charging station. Such a case would require a human intervention to make TIM operational again and this is not acceptable since it could require to postpone or stop the operation of the LHC.

On another hand, the second main issue is the fact that the speed of the train is imposed by a controller which do not take into account the environment, the mission length and do not verify a priori if the energy remaining in the battery is sufficient to reach destination. This last task is currently ensured by the operator which could lead to appreciation error and to fully drained batteries before the end of the mission since the operator is not necessarily a trained expert.

In the next parts of this document, it will be shown how these issue has been tackled by implementing a more accurate SOC estimation in order to know as accurately as possible the amount energy remaining in TIM batteries, a mechanical model targeting at providing an a priori estimation of the amount of energy needed for mission completion and an non-linear optimization system aiming at reducing the overall consumption of this train.

1 Table of contents

2 Introduction

2.1 Presentation of CERN

CERN, “Centre Européen pour la Recherche Nucléaire” or “European Organisation for Nuclear Research”, is considered as one of the world’s largest laboratory for scientific research. Located in the area of Geneva on the border between Switzerland and France, it has twenty European member states. Nevertheless, scientists coming from non-member states can collaborate with CERN, making it one of the most multicultural working environments. Established in 1954, CERN has achieved several important discoveries since its creation, leading among others to two Nobel prizes in physics and the invention of the World Wide Web.

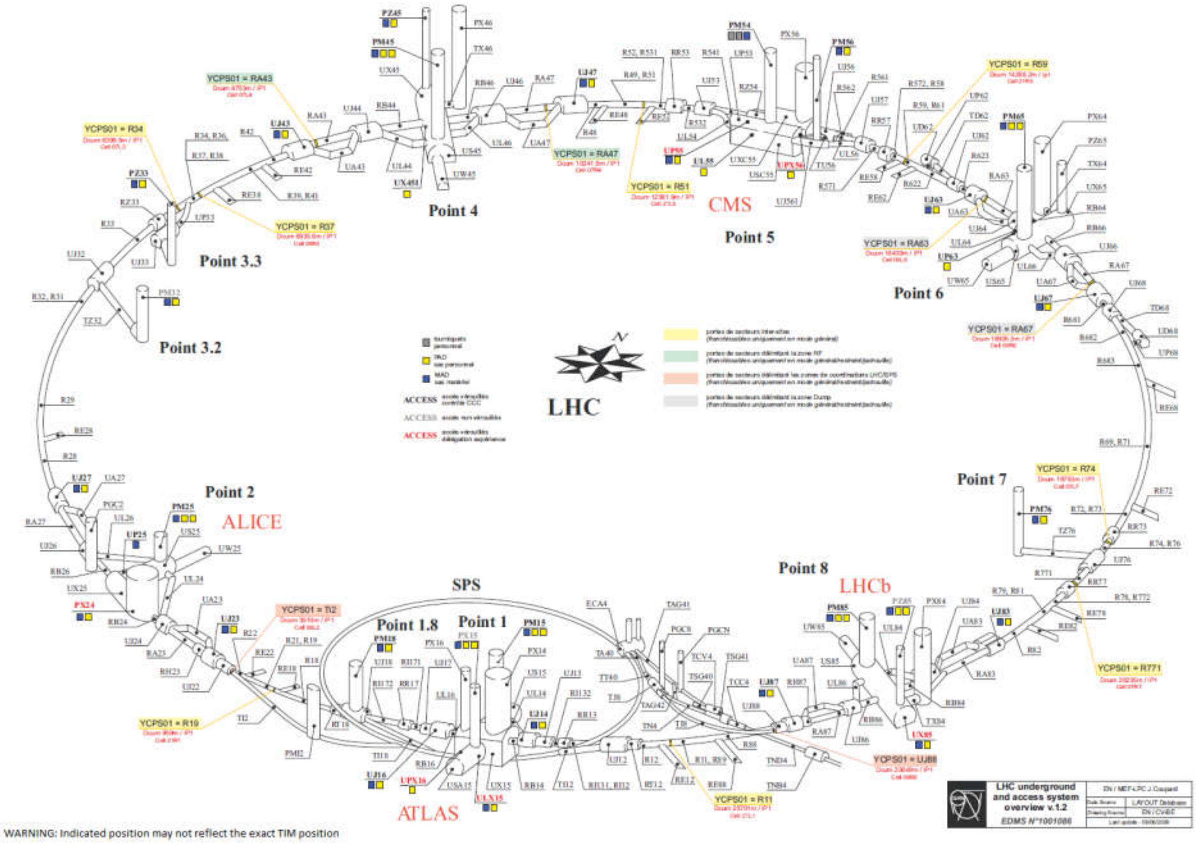

Figure 1: LHC Tunnel representation (not scaled)

Currently, more than 12000 scientists (belonging to 120 different nationalities) are collaborating at CERN which main function is to provide the particle accelerators needed for high-energy physics experiments. As a result, numerous experiments have been constructed at CERN. Around the construction and the maintenance of the accelerators, a lot of research is done involving medicine, engineering and computer science in order to provide the best research installations. The main instruments used at CERN are particle accelerators and detectors. Accelerators boost beams of particles to high energy levels before the beams are forced to collide with each other. Detectors observe and record the results of these collisions, from which physicists study the particles emitted from high energy collisions [1].

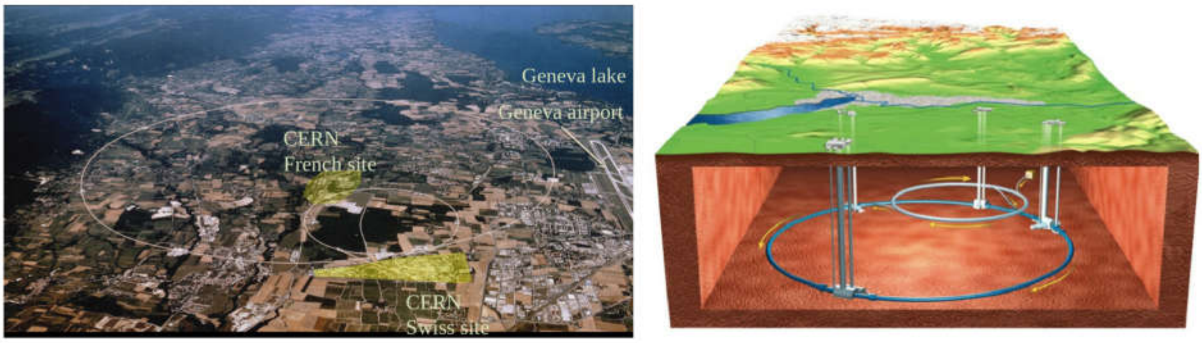

Figure 2: CERN site viewed from above (left) and visualization of underground installations (left).

2.2 Presentation of the Robotronic Section

CERN's experiments involve colliding particles beams together. When this happens some of the particles release radiation. Radiation only occurs at CERN when the particle beam is on, and turning it off stops the emissions immediately but materials surrounding installation are exposed and can remain radioactive even if the beam is off. Since the LHC experiments are on average 100m underground, this provides a natural barrier to radiation. This does not prevent workers intervening in the tunnel from being exposed to remaining radiations and remotely controlled mobile robots, able to carry out maintenance work and inspections, are now considered for applications in hostile and hazardous environments in order to reduce the human intervention and radiation doses absorbed by workers. One will note that every worker accessing critical areas is equipped with a dosimeter which monitors the dose of radiation worker is exposed to and once annual dose (far below EU standards) has been reached, the worker cannot be exposed during a determined period in order to ensure his security

The Robotronic section at CERN is aiming at minimizing the hazardous exposition by developing tele-operated solutions that give the possibility to replace partially or totally human interventions by, for example, sending a tele-operated robot, equipped with robotic arms, to perform maintenance intervention. Development of such solutions gather several fields of engineering such as mechanical engineering, electrical and electronic engineering, process-control engineering, robotic oriented programming and communication. In addition, the robotic solutions developed must always be resistant to harsh environment of the underground installation in such a way that the risk of breakdown is minimized. Also, harsh conditions of operation must be taken into account at all stages of the design. Indeed, once the experiment has started, it becomes very difficult to go on site and repair or modify installations inside the tunnel without exposing workers to radiations.

One of the robotic solutions designed by the EN-STI-ECE section to overcome radiation exposition problem, is the Train Inspection Monorail (TIM). This robot can travel along the tunnel on a monorail attached to the tunnel's ceiling and perform all kind of measurements such as radiation oxygen and temperature levels measurement, visual inspection and telemetry of collimator alignment. In the future, the TIM will be also able to carry a robotic arms on its payload wagon and to perform mechanical intervention on tunnel installations [1].

2.3 Presentation of the Train Inspection Monorail

2.3.1 TIM general information

The Train Inspection Monorail (TIM) is an in-house CERN product with a goal to provide unmanned actions in the LHC tunnel when there is no active beam (during the beam stops and shut-downs). The effort for the manual measurements of the LHC components is enormous. Remote measurements can be made even during tests when the access to the LHC tunnel is not allowed to humans. The implementation of new measurement units to TIM has the goal of minimizing the dose of the personnel performing the measurements.

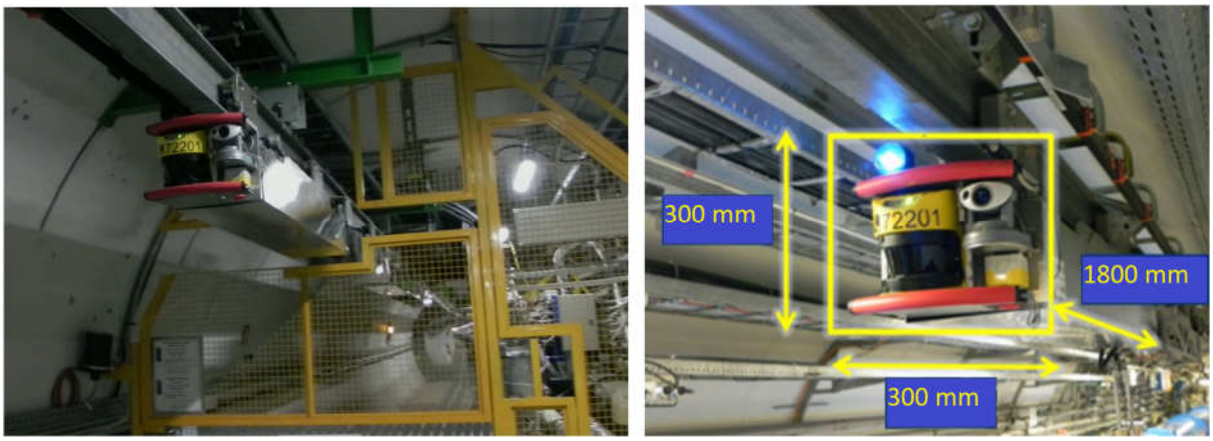

Figure 3: TIM in the LCH

The TIM is a remotely controlled inspection train designed to be a modular system currently made up of 5 wagons. Each wagon has a dedicated task. The payload wagon is the one that can be modularly replaced and adapted depending on the needs of the missions. Each Wagon is equipped with a PLC ensuring the control of devices and communication with others wagon. The “reconnaissance” wagon also embed and Industrial PC (IPC) mainly used for communication and for recording data acquired during missions. Figure 4 schematically represents the organization of the wagons TIM is made of.

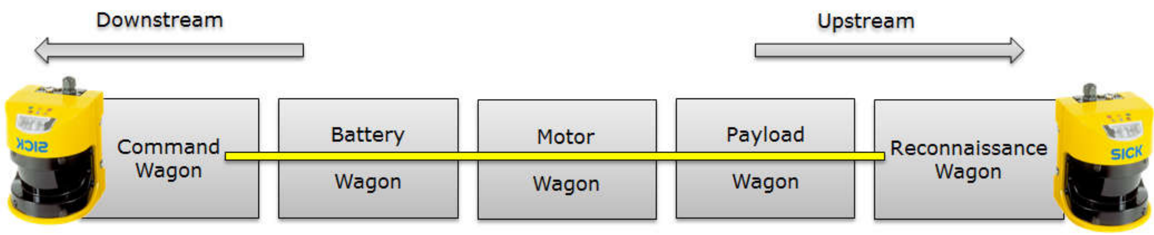

Figure 4: TIM wagons layout

2.3.2 Communication with TIM

The communication with the train is one of the critical part of the system since if a communication loss occurs, the operator is no longer able to send commands to the train and has absolutely no feedback on TIM behavior. This is why TIM should be totally autonomous and operate in a stand-alone way once its mission has been received.

In order to minimize communication errors between each wagon which would disable TIM autonomous capability, the internal communication of the train is ensured by mean of a PROFIsafe/PROFInet network. This industrial standardized protocol for critical applications is based on Ethernet links ensuring the transmission of the data with error control, failure detection and source/destination authentication. It has been proven reliable and is used in many systems where security and reliability of communication is mandatory.

On the other hand communication with surface can be achieved by two ways:

- Command and reconnaissance wagons both have, for redundancy reasons, a 4G modem which can be accessed through a VPN over a 4G network presents in the tunnel.

- Command and reconnaissance wagons both have, for redundancy reasons, a WIFI router which can be accessed over CERN network when the train is in areas of the tunnel covered by WIFI.

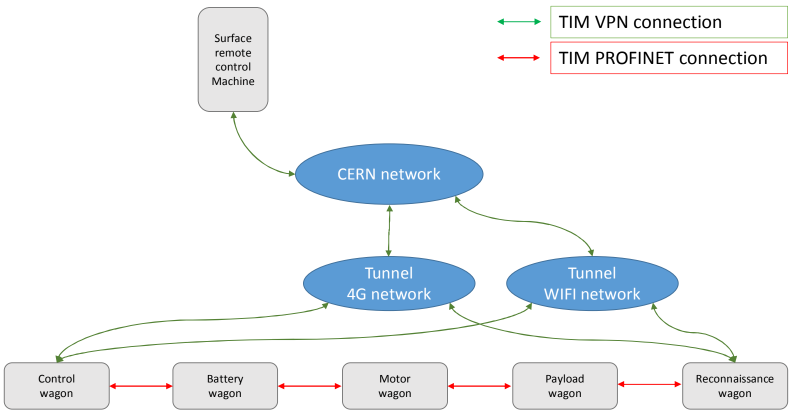

The communication with the surface cannot be considered as reliable in the way that, losses of communication can possibly happen. Indeed, when communication is based on non-wired connections, the risk of loss of communication is always more important than with wired ones. Moreover in such an intricate location as a tunnel 100m under ground level and in the vicinity of a 360MJ particles beam, the probability of communication loss increases drastically.

2.3.3 Remote control

The GUI of the TIM has been designed with LabVIEW and is running on a server connecter to CERN the network. It allows the operator to manage the train movements and to plan several kind of missions. Additionally, the interface gives a visual feedback using the embedded cameras on the train, as well as a feedback on all the important data that the user should be aware of during the operation. This interface has been designed for being user friendly without having the need of overly trained operators. One of the views of the GUI can be seen on Figure 5.

2.3.4 Project useful measurements.

The measurement of the train position is based on a free-running wheel that pushes against the rail. As there may be some slippage, the rail is also fitted with barcoded labels at known locations. The train can correct the position it computes with the wheel based on the bar codes it scans. This results in a positioning system with an accuracy of less than 1 cm.

Also electrical measurements are performed by the PLC of the battery wagon which can, via a LEM Hall Effect sensor and a voltage transducer, measures respectively the current consumed by the train and the battery voltage.

Last a SOC estimator provided by Hoppecke return estimations of the amount of energy remaining in the battery but this measurement is not considered as accurate and should not be taken into account.

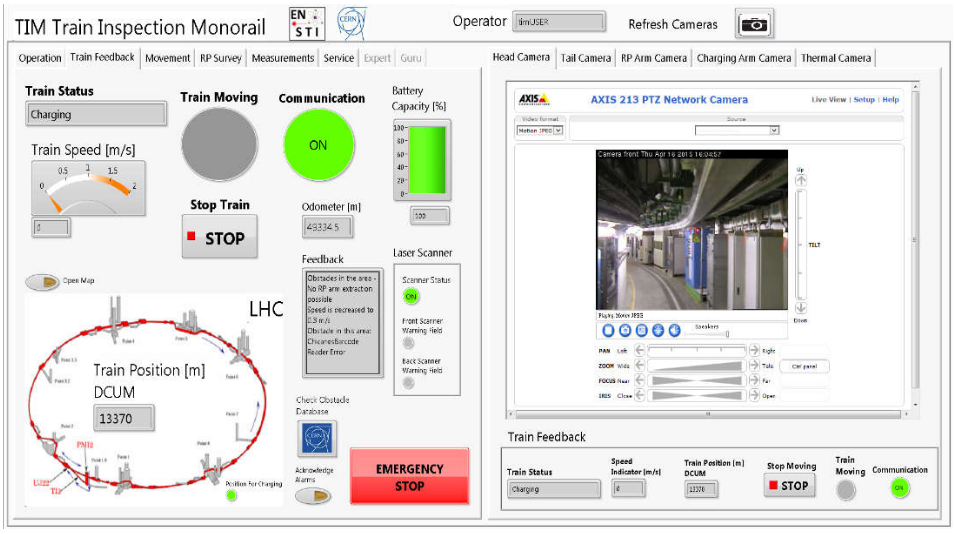

Figure 5: Overview of the TIM LabVIEW GUI

The TIM train and its software have been designed for being robust and reliable. A special emphasis on safety in order not to harm any equipment or personnel has been taken during all the development process. TIM intelligence makes the system able to perform the measurement missions completely autonomously once the operator has introduced the mission configuration. After mission completion, data logged are stored in a database and displayed on the internal CERN website designed specifically for TIM measurement display.

New features for TIM are being developed at CERN since different applications want to take advantage of its safety, robustness and accuracy in position. For example, after the installation of a specific camera that can capture images while the train is moving, an autonomous image processing system is being developed in order to be able to compare two pictures, taken in two different moments in time, and detect possible anomalies of the tunnel infrastructure. Another project, is aiming at placing two robotic arms on the payload wagon in order to perform tele-operated mechanical maintenance or repair interventions.

Figure 6: Camera placed on a retractable arm (left) structure of the tunnel (right)

TIM main characteristics

The system characteristics are subject to change since TIM is in constant evolution. But current main values are summarized in Table 1.

Communication	Remote operated via 4G LTE or over WIFI in covered areas of the tunnel
Security Level	SIL 2
Total length	10.2 m
Overall dimensions (1 wagon)	(1800x300x300) mm
Number of wagons	5
Total weight (current configuration)	~600 kg
Maximum speed	6.5 km/h = 1.80 m/s
Supply voltage (power rail)	230/400 VAC
Operating voltage (2 batteries)	24 V DC (2x12 V)
Battery	150Ah @ C20 lead-acid
Power consumption in idle state Economy mode / normal mode	57W / 185W
Power consumption during mission Min/max	185W / 1600W
Autonomy (estimation @ full speed)	~20 km

Table 1: Main TIM characteristics

3 Battery pack characteristics

The choice of the batteries for an electrical vehicle is the basis of the design of the power train since the performances of the vehicle will depend on batteries capabilities. Indeed, batteries must be capable of suppling actuators such as motors which can demand high transient. In addition batteries provide the power needed to feed on-board control electronic devices which requires stable voltage within a determined range. Also the battery bank total capacity must be sized properly in order to ensure an operation duration as long as possible. Thus, according to generally reduced space available in the on the vehicle and the limitations on the embedded weight, the proper threshold between power density and energy density must be found.

Figure 7: Varta battery installed on TIM

TIM is powered by lead acid batteries using Absorbent Gel Material (AGM) technology. This technology is suitable for TIM application as it has been proven reliable, safe and it is in use since early 80’s in the military. Moreover, the model of battery chosen can accept deep discharges without noticeable capacity losses. This technology provide a good compromise between power and energy density and resists very well to vibrations TIM can generate since the gelled sulphuric acid electrolyte is made of is contained inside porous glass fiber which prevent it from moving inside the battery and spilling out. Even if other technologies would provide better performance, for instance, lithium titanate technology, the chosen Lead-Acid battery offers the advantage of do not needing a cooling system and relatively simple system for security. Indeed, it has been considered changing the battery technology in order to increase the total battery bank capacity and decrease charge period by designing a brand new lithium titanate battery bank but this solution would have implied to design a battery control system for ensuring safety which would have required extra costs and time which were not available.

The Train Inspection Monorail can be equipped with 2 different battery models: the VARTA LAD 150-12V batteries which were originally installed, are no more available since their production has been discontinued. Batteries reaching end of life will be pre-emptively replaced with BANNER GivC 12-150 as soon as access to the tunnel will be granted.

<u>Constant discharge characteristics</u>

Electrochemical batteries have a particular behavior and cannot be seen as energy storage system with fixed capacity. As a matter of fact, the amount of available energy is decreasing non-linearly with the increase of constant discharge current. Figure 8 and Table 2 represent both battery types characteristic

One can notice that new batteries bring a bit increase on the performances; as it can be seen on Figure 8 , banner batteries keep a higher constant discharge capacity for higher discharge currents. The only drawback is that these differences between the characteristics must be taken into account in the next developments, each algorithm presented latter on in this document has to be tested with both battery types.

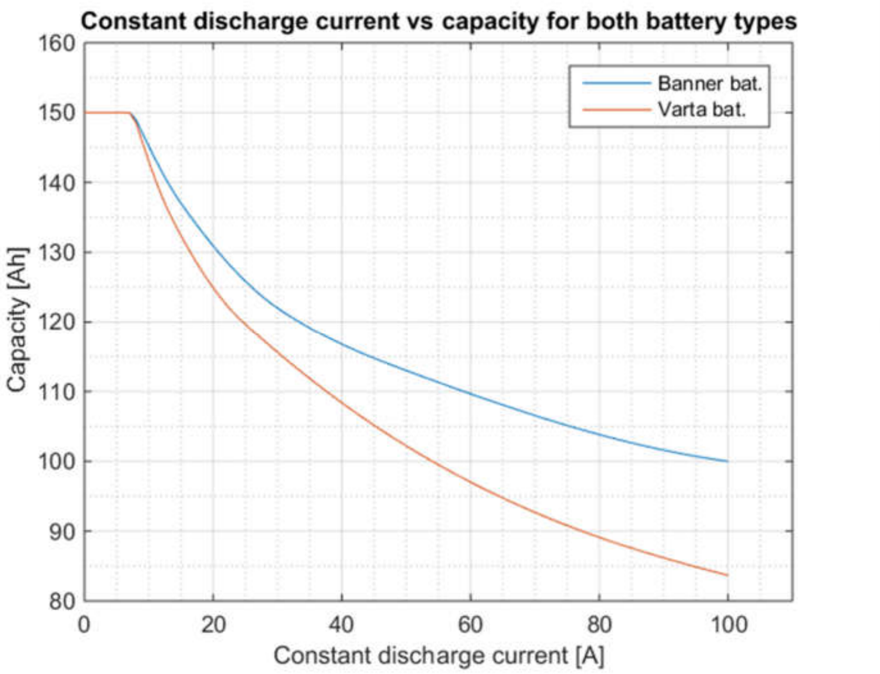

Figure 8 Constant discharge capacity for both battery types (provided by suppliers)

Batteries characteristics	VARTA LAD 150 12V	BANNER GivC 12-150	Units
Voltage	12	12	V
End of Discharge Voltage	10	10	V
Rated capacity C20 (@ 7.5A)	150	150	Ah
Capacity C10 (@ 15A)	123	137	Ah
Capacity C5 (@ 30A)	115	122	Ah
Capacity C3 (@ 50A)	102	113	Ah
Capacity C1.5 (@ 100A)	83	100	Ah

.

Table 2: Constant discharge capacity data

Each TIM train (currently 2 installed on LHC) are each equipped with 2 batteries mounted in serie and provide a reserve of energy of 300Ah in total. Since the tests presented in this work has been performed on 1 battery at a time and since the same current is flowing through both batteries, it will be assumed that both batteries are equally discharged when a load is connected to the positive and negative terminal of the pack of two batteries. This assumption is valid as long as there is no current leak at the interconnection of the two batteries. Furthermore, the SOC estimator presented later on has been calibrated for 1 battery and this assumption also involves that the initial SOC and the one during discharge are equals on both batteries taken separately.

4 State-Of-Charge estimation

When dealing with battery powered vehicles and with battery powered devices in general, one of the crucial points related to the autonomy and reliability of the system is to determine which percentage of the initial energy is remaining stored in the battery. The system has to know at each instant, knowing approximatively the cost of these, how many kilometers or energy consuming actions it will be able to perform with the energy still available in the power bank. In order to solve this issue and since the TIM is only equipped with a very basic SOC estimation system (Hoppecke sensor) which provides non accurate and overestimated values of the SOC, a new system able to provide reliable and more accurate estimations, has to be implemented on TIM.

4.1 Definitions

The number representing the amount of energy remaining in the battery with respect to rated capacity is called State-Of-Charge or SOC for short.

It is defined as:

$$SOC\left[pu\right] = \frac{Available\ Capacity\ \left[Ah\right]}{Rated\ \ Capacity\ \left[Ah\right]} \quad with:\ 0 < SOC < 1$$

NB1: One can indifferently express the SOC in percent by multiplying SOC in per-unit by 100
NB2: This formulation considering a constant rated capacity is true if we consider an ideal battery. This would imply a constant capacity independent of the discharge rate which is not true at in real world.

In opposition to SOC, one can also define the Depth Of Discharge (DOD) which represents the energy spent since last full charge of the battery.

$$DOD\left[pu\right] = \frac{Energy\ Spent\left[Ah / As\right]}{Rated\ \ Capacity\ \left[Ah / As\right]} \quad \text{with DOD>0}$$

The DOD is not bound by the upper 1 [pu] limit since it can happen that the actually spent energy is higher than the rated capacity of the battery (especially if the whole discharge is done with a current lower than C/5 which is the value at which the rated capacity should be defined).

SOC value which apparently seems to be easily calculated cannot be straightforwardly deduced and some specific methods has been developed. Main methods will be quickly explained in next section as a reminder and to justify choices that has been done.

4.2 Most common SOC estimation methods

Several methods aiming at estimating the SOC of a battery has been developed since batteries has been discovered. Some of them will be quickly explained in order to highlight the reason that lead to the choice of the implemented SOC estimator. Furthermore, it will be also explained why these methods are not applicable to TIM batteries.

Current integration method:

This method consists simply in integrating current taken from the battery at each algorithm iteration and subtract the value obtained from the SOC at previous step. This method is also known as the “Coulomb Counting Method” since it is implicitly counting the coulombic charges extracted from the battery. This method could applicable to TIM batteries but the main drawback of this method is the lack of accuracy since it considers that the capacity of the battery remains constant (independent from current) which is incorrect and induces huge deviations from actual SOC.

Specific gravity method:

It can be possible to measure the amount of acid in the battery electrolyte by means of the specific gravity measurement. When the electrochemical reaction happens in the lead-acid battery, the sulphuric acid is decomposed on lead anode and cathode and its concentration inside the electrolyte decreases with the SOC. This measurement indicate the state of the electrochemical reaction in the battery and if the original composition of the electrolyte is well known this method provide good result but it is simply not applicable to most applications and to TIM in particular. Indeed, this measurement must be done after resting the battery for a while (the recombination inside the battery must be completed) which prevent from having an instantaneous SOC estimation. Moreover, it involves human intervention (which is precisely what TIM is trying to minimize) to withdraw a sample of electrolyte from the battery and perform the specific gravity measurement.

Open circuit voltage method:

The open circuit voltage (OCV) is dependent on the SOC of the battery. Also it can be possible, knowing the characteristic SOC vs OCV, to estimate the amount of energy remaining in the battery. The major drawback of this method is that the battery has to be rested (with a zero current discharge) for some time before measuring voltage which do not allow inline measurements (when current is being taken from the battery).

Several other methods exist but since these are neither not applicable to the TIM system, these are not explained in this section.

The SOC estimator that has been implemented on TIM must be able to continuously provide an estimation and to do not interrupt train’s operation. Thus the method the most likely applicable in the Current integration method but since this latter provides non accurate results, a more accurate method has to be found in order to be able to compute SOC in “real-time”.

Since none of the above mentioned methods suits the constraints and requirements of the TIM system, one has to find another and more sophisticated way to estimate the amount of energy remaining available in TIM battery bank.

4.3 SOC estimator chosen

In order to achieve a satisfying accuracy on SOC estimation, an improved version of the Current Integration Method has been chosen. This method detailed in [2] and [3], is aiming, in the end, at being implemented on the Programmable Logic Controller embedded on the battery wagon. This method has the advantage to take into account the variation of the battery capacity according to discharge current which leads to a significant increase of the accuracy of the estimation. This SOC estimation method is also perfect for TIM system since it does not require excessively complex computations and it can be run on the PLC embedded but more importantly, this method do not need to interrupt battery operation and an estimation can be computed “in line” at a relatively high frequency compared to the TIM current consumption dynamic. The measurements of current taken from battery is acquired by the PLC at a frequency 10Hz. This acquisition frequency allows to be able to capture transient phenomenon during accelerations/decelerations which time constant is in the order of 1 second (overshoots of current during typical acceleration from 0 to 1.8m/s lasts around 6 seconds). This guarantee, that transient phases are taken into account by the estimator.

The formulation of the algorithm [2] implemented is quickly presented below and formulated as:

$$SOC(\mathrm{t}) = \frac{C(\mathrm{t}-\Delta\mathrm{t}) - \alpha(\mathrm{I},\theta).\left(\mathrm{I}(\mathrm{t}-\Delta\mathrm{t}) + \mathrm{I}(\mathrm{t})\right)\frac{\Delta t}{2}}{C(\mathrm{I}_{cts},\theta)}$$

With :

$$C(\mathrm{t}-\Delta\mathrm{t}) \;=\; C(\mathrm{I}_{cts},\theta).SOC(\mathrm{t}-\Delta t)$$

And where:

- SOC is the State Of Charge
- $\mathrm{I(t)}$ is the instantaneous current measurement $[\mathrm{A}]$
- I_{cts} is the current filtered using a moving average (typ. length T= 5-10s or N=T/Δt samples) $[\mathrm{A}]$
- $\alpha(\mathrm{I},\theta)$ is the charge/discharge efficiency $[-]$
- $C(\mathrm{I}_{cts},\theta)$ is the capacity w.r.t. constant discharge current and batt. temp. $[\mathrm{As}]$
- Δt is the loop period of the estimator $[s]$
- θ is the battery electrolyte temperature assumed 30°C (since not available) $[°C]$

Compared to the well-known “Coulombic method”, the State-Of-Charge at time t, now not only depends on Current (one or two last values depending on integration method) and SOC at previous iteration but also on N previous samples of the current extracted and on the characteristics of the battery. Indeed, N last samples are averaged and given, along with electrolyte temperature, to an interpolation function of the constant current discharge characteristic that returns the Constant Discharge Capacity: $C(\mathrm{I}_{cts},\theta)$. These implies a more sophisticated estimation than the simple “Coulomb counting” method and additional computations but it will be shown latter on that the accuracy of the estimation is hugely improved thanks to this mechanism.

A representation of how this algorithm has been implemented is shown on Figure 9. It has been adapted to several targets: the PLC embedded on TIM, the myRIO of the battery test bench and in Matlab and all these implementations return similar results. Nevertheless, only implementations on PLC and on myRIO are real time implementations. The one on Matlab is aiming at post processing of logged data and is not executed in real-time. Indeed, the matlab implementation has been used with logged data of current and corresponding sample time information in order to compare with values provided by PLC and myRIO implementations.

The Matlab script has been optimized using as much as possible vectorization. As a result, it can generate the SOC estimation profile for each iteration step of 20ms of a 5 hour long discharge (almost one million values) in less than 2s (approx. 2µs/pt). Of course the computation time highly depends on the machine on which it is executed but is provide huge improvement since same computations performed without optimization were taking more than 1min.

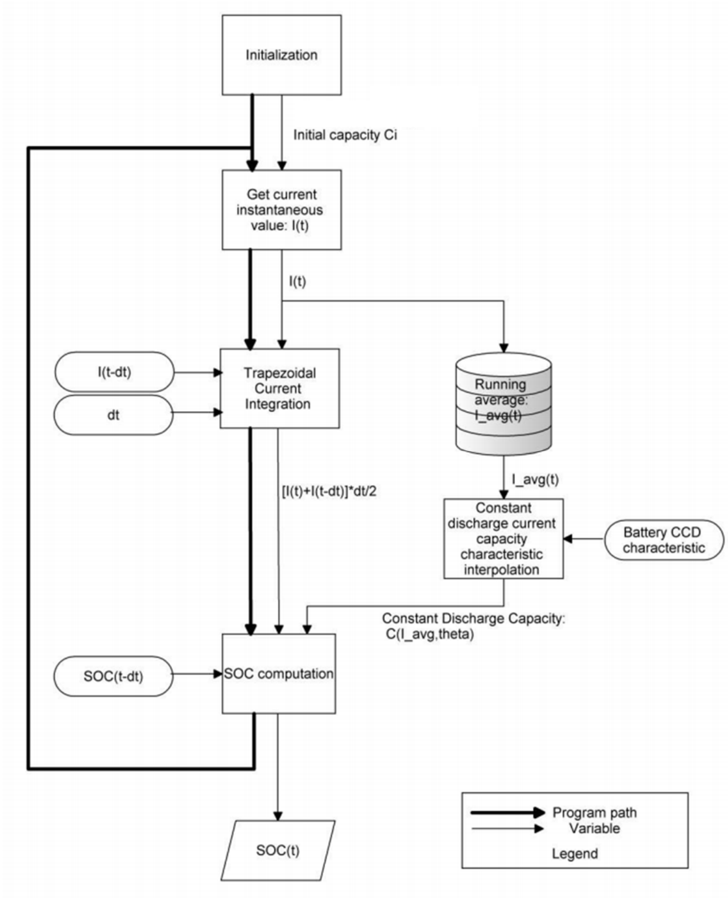

Figure 9: SOC estimator Principle

4.4 SOC estimator validation

In order to have an idea of the quality of the values provided by the SOC estimator, a specific procedure has to be set up. This measurement of the accuracy is mandatory as the whole reliability of the train relies on this estimation. Indeed, it would be a real problem if it happened that the train battery went completely empty in the tunnel, preventing any movement and communication and requiring a human intervention to fix it, which is precisely what TIM is supposed to avoid.

Since the verification involve a complete discharge of the battery, the tests last for hours and in order to avoid doing it manually, it has been chosen to design a test bench to make the process automatic. This section will describe the test procedure and detail the test bench design and control.

4.4.1 Procedure

This test procedure is aiming at three main goals. First one is to provide values of the real SOC at defined instant during discharge in order to compare it with the true SOC and tune the parameters of the estimator to reach the maximum accuracy. Second goal is to quantify the error on the SOC for different values such as an information on the reliability and quality of the estimation can be deduced. Third and last goal is to have the ability to perform battery capacity measurement in order to determine the battery health. For that last particular case, the whole discharge has to be performed at a constant discharge rate.

When an initially fully charged battery has started to be discharged, the only reliable way to know how many energy is remaining inside the battery is to discharge in totally until voltage between the terminals reaches a minimal value. This values is called the End Of Discharge Voltage (EODV). In normal conditions, battery voltage should never go below EODV since it could result in irreversible damages, it accelerates ages and quickly reduce the capacity.

The test procedure is a sequence of two states. First starting with a fully charged battery, a predefined current profile is absorbed by the DC electronic load in order to simulate a typical current consumption. Then once battery has been discharged for a specific amount of time and the estimation algorithm has provided the values of the State-Of-Charge, the constant discharge phase begins. This constant discharge is performed at the industry standard value of C/5 (e.g. 30A for TIM battery). The current must be maintained until the voltage at battery terminals reached the EODV. This indicates that the battery is fully discharged and the current is then set to zero. One will notice that even if the EODV is reached, current can still be provided by the battery. This means that energy is still available but if the discharge continues, the battery is brought outside of the normal operation limits and damages can occur.

4.4.2 Design of the test bench

In order to perform the above mentioned tests on TIM batteries, a new test bench has been designed. This latter must have the ability to measure and record not only the current flowing through the battery but also the voltage between its terminals. It must also give the possibility to control accurately the current provided by the battery.

The principle of the solution adopted in order to satisfy the constraints of the tests, is shown on Figure 10, whereas the practical realization can be seen on Figure 12. 3

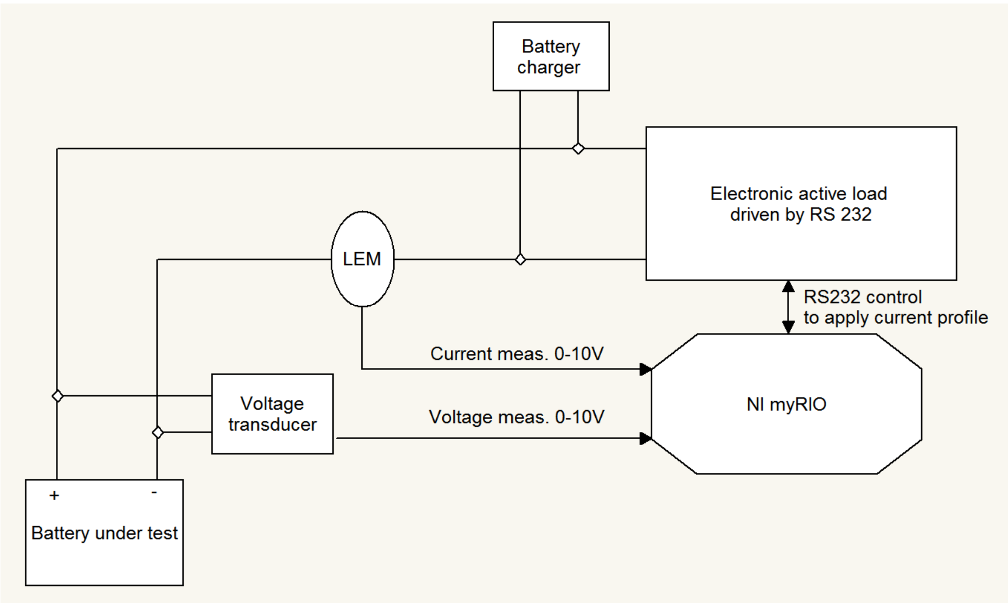

Figure 10: Battery test bench layout

The controller of the test bench is a myRIO from National Instruments, this device perfectly fits with the requirements of the test bench since it provides a good computational speed, analog inputs and a RS232 communication capability just by adding a USB/RS232 converter. The program designed and running on the myRIO ensure the data logging, the DC electronic load control via RS232 communication, the test sequence control and the real-time SOC estimation.

The Graphical User Interface (GUI), running on a computer connected to the myRIO, used by the user of the test bench can be seen on Figure 11. It allows to configure the parameters of the test to be performed, such as the EODV, the SOC value for which the constant current discharge begins and the main characteristics of the battery.

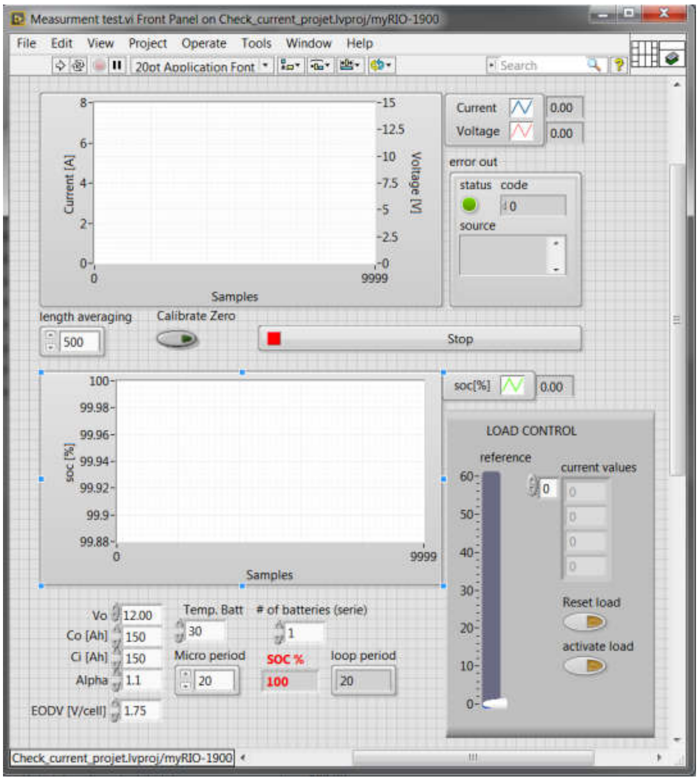

Figure 11: GUI of the test bench

Figure 12: Test bench, real installation and control GUI

Below are listed interesting characteristics of devices the Test bench is made of in order to give an idea of performances that can be achieved.

DC electronic load N3300A:

Power: 2*150W plus 2*300W channels in parallel (max. peak: 900W)

Current @ 14V: 0 - 60A

Accuracy on current regulation: 8mA

Control mode: RS232

Hall effect LEM sensor DHR 100C10:

Input range: 0-100A

Accuracy: 1%

Output: 0-10V

Voltage transducer MACX MCR VDC:

Input range: +/- 36VDC

Accuracy: 1%

Output: 0-10V

NI myRIO:

Dual-core processor frequency: 667 MHz

RAM: 256MB DDR3

12bits analog +/-10V inputs at a rate of 500 kS/s

Accuracy on +/-10V AI: 2%

USB2.0 to RS232 drivers available

Battery Charger:

Output voltage: 12-14.7V

Output current: 0-10A

Special charging mode for AGM batteries

4.4.1 SOC algorithm validation procedure

The SOC estimation algorithm accuracy can be evaluated using the test bench presented above. The idea is the following: knowing the amount of energy stored in the battery at the beginning of the test (rated capacity of 150Ah for a fully charged battery), the algorithm is initialized with this value lead to a SOC equals to 1. Starting from this, the battery is discharged over a predefined period with a current varying within the typical current range consumed by TIM [7 to 35A]. At the end of this first phase, the SOC provided by the estimator, SOC_1^{est}, is stored and the varying current consumption changes becoming a constant current consumption at a standardized discharge rate of C/5 (30A) until the voltage between battery terminals reaches the EODV (10V for both batteries). Then the current is set to zero and the test is stopped.

The way the estimator has been tested corresponds to the way the estimator will be used on TIM. Indeed, the train stays, most of the time, under charge which means that when user starts using it the mission always begin with a fully charged battery pack or with a partially charged battery bank on which only one partial discharge has been performed.

During the whole duration of the test, battery current, battery voltage and time are logged inside a text file at a loop iteration period of $\Delta t = 20ms$. This allows to apply a post processing on the data logged in order to compare the value of SOC_1^{est} with the true remaining SOC obtained.

The true remaining State-Of-Charge SOC_1^{true} is obtained with:

$$SOC_1^{true} = \frac{1 - \int I_{cte}(\mathrm{t})\,\mathrm{dt}}{C_{@30A}}$$

where:

$\mathrm{I}_{cte}(\mathrm{t})$: the evolution of the current during constant discharge phase (30A)

$C_{@30A}$: battery capacity for a constant discharge rate equals to C/5 (30A)

Since during the constant discharge phase, I_{cte} and $C_{@30A}$ have constant values, the expression of SOC_1^{true} could be simplified but this simplification has not been used in order to ensure the validity of the computation and to take into account potential current deviations (which practically do not occur).

Once the value of SOC_1^{true} is known, it can be compared with the value of SOC_1^{est} by relative and absolute error determination:

Absolute error is given by:

$$\varepsilon_{soc}^{abs} = \left| SOC_1^{true} - SOC_1^{est} \right|$$

Relative error is given by:

$$\varepsilon_{soc}^{rel} = \frac{\varepsilon_{soc}^{abs}}{SOC_1^{true}} * 100$$

NB: here subscripts 1 indicate that these SOC are the one at the end of the 1st discharge phase (non-constant discharge).

These error have been computed for each discharge test and put into relation with the Depth-Of-Disharge in order to allow the estimation of the quality of the values provided by the SOC estimation algorithm.e

4.4.2 Tuning of the estimator

In order for the SOC to provide as accurate estimations as possible, the parameters of the algorithm has been empirically tuned. The parameters to be tuned are typically the running average length and the efficient coefficient of the battery. Reader will note that the temperature of the electrolyte of the battery only has a limited impact on the algorithm estimation accuracy and will be considered constant (20°C) because the type of battery used on TIM system does not provide access to electrolyte (sealed maintenance free battery).

The tuning of the parameters of the estimation has been performed manually by finding the best thread-off between running average length and charge/discharge efficiency.

Best results has been obtained with values that can be seen in

Table 3

	Varta bat.	Banner bat	Units
Charge/discharge efficiency	1.2	1.1	[-]
Running average length	5	5	[s]

Table 3: Values of parameters minimizing SOC estimation errors

4.5 **Results:**

<u>Typical test results:</u> (full sets of test results and further analysis can be seen in appendices)

The measurements and analysis performed on the SOC estimator show a relatively good accuracy for one discharge cycle. Indeed, the biggest relative error obtained is 1.8% for a Depth-Of-Discharge of 68%.

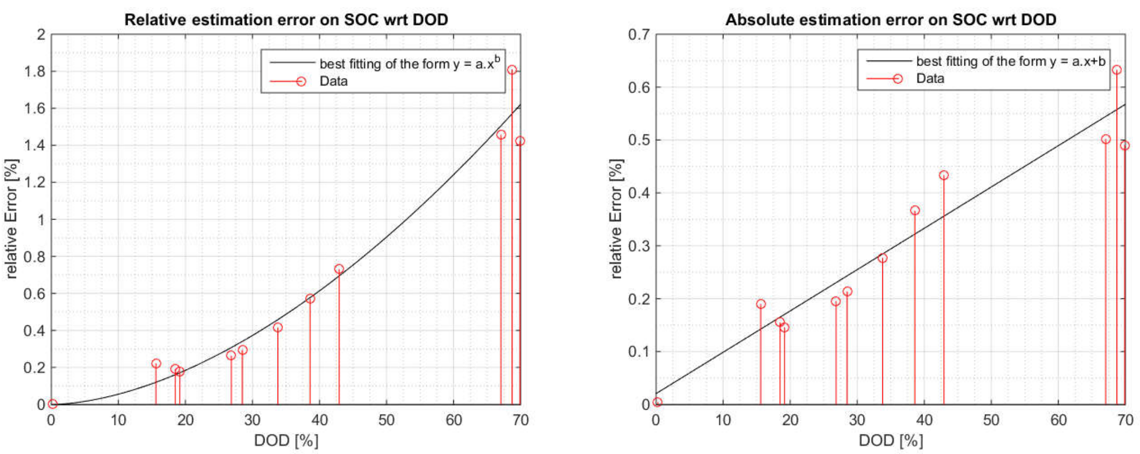

Figure 13: Relative (left) and absolute (right) error wrt Depth-Of-Discharge

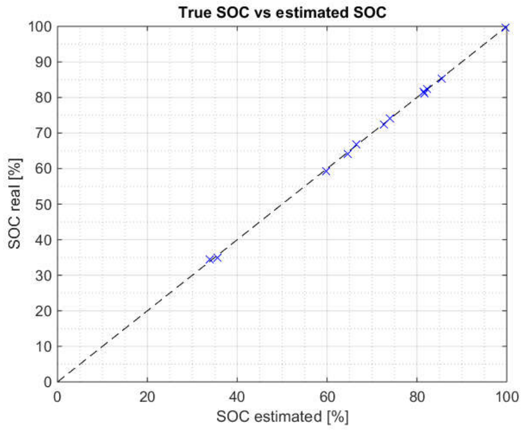

Figure 14: Comparison of real SOC vs estimated SOC

These results have to be interpreted with care as they correspond to only one discharge cycle. In order to have a little bit more complete results, it could have been useful to perform several partial charge/discharge cycles in order to see the behavior on the SOC estimator but since this error quantification method resemble to the real conditions of use of the batteries, these results are satisfying for this specific usage of the batteries since deviations are relatively small when comparing the SOC estimated and the true one as it can be seen on Figure 14.

Real current profile test result:

A test performed by applying a real current profile logged during a mission has been done. The procedure to quantify the energy left still stored in the battery is exactly the same as in previous test but the current profile of the 1st discharge phase has been replaced by real measurements as if TIM was actually consuming the current during a real mission.

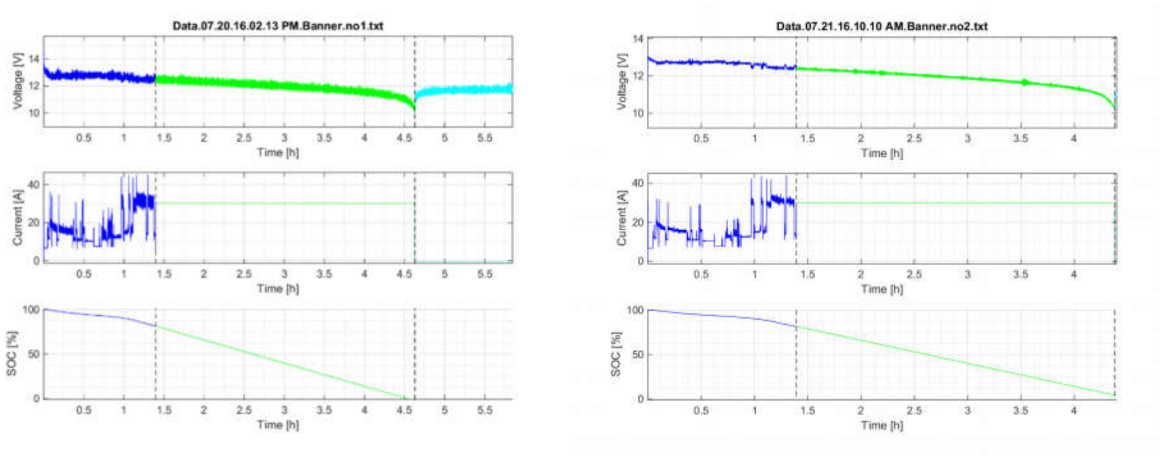

Figure 15: Real current profile discharge test on 2 different Banner batteries

Banner battery

Data_07_20_16_02_13 PM_Banner_no1.txt

Total test duration: 4.6287 h
Total energy extracted: 120.3247 Ah
Energy extracted during 1st phase: 23.0337 Ah
Energy extracted during 2nd phase: 97.6249 Ah
Depth Of Discharge after 1st phase: 19.143 %
SOC real after 1st phase: 81.1199 %
SOC estimated after 1st phase: 81.6444 %
SOC estimation error: 0.64661 %
SOC estimation at end of discharge: -2.452 %

Elapsed time is 1.989289 seconds.

Banner battery

Data_07_21_16_10_10 AM_Banner_no2.txt

Total test duration: 4.3801 h
Total energy extracted: 112.7286 Ah
Energy extracted during 1st phase: 22.9936 Ah
Energy extracted during 2nd phase: 89.7357 Ah
Depth Of Discharge after 1st phase: 20.3973 %
SOC real after 1st phase: 81.1528 %
SOC estimated after 1st phase: 81.6816 %
SOC estimation error: 0.65163 %
SOC estimation at end of discharge: 4.4317 %

Elapsed time is 1.611233 seconds.

This test, performed on the both available Banner batteries (the one supposed to replace Varta batteries installed on TIM) give similar results with relative error on SOC estimation at the nd of the 1st phase of respectively 0.647% and 0.652%. It is a clear indication that the estimations provided are reproducible even on two different batteries of the same supplier. Of course in order to give more information on the accuracy of the estimation with real current profiles, it would be relevant to perform further tests with several sets of data but these were not available since the missions in the tunnel were not allowed during almost all the duration of this work. Moreover, time required to perform further test was not available.

It can be stated that the estimation of the SOC provide by the algorithm are quite accurate and the implementation of the algorithm provides reliable estimations if the batteries are fully charged before the beginning of the discharge.

5 TIM current consumption model

In order to formulate the energy consumption optimization problem presented later on, it is needed to find a way to simulate the behavior of the train. This section aims at presenting how the model has been identified and how it can be used to predict the energy needed to perform a mission before moving the train.

At first, it has been thought that is could be possible to model the train behavior by writing down movement equations of the system but after several attempts, it has been noticed that the complexity of the mechanical system, the approximation induced and the irregularities of the rail could not lead to a relevant and accurate description of the mechanical behavior of the train. Thus it has been chosen to develop a system that could automatically identify given data acquired during train operation, in order to describe the behavior of particular components of the model that cannot easily be described with usual theoretical formulation ($F_{fr} = a+b.v+c.v^2$)..

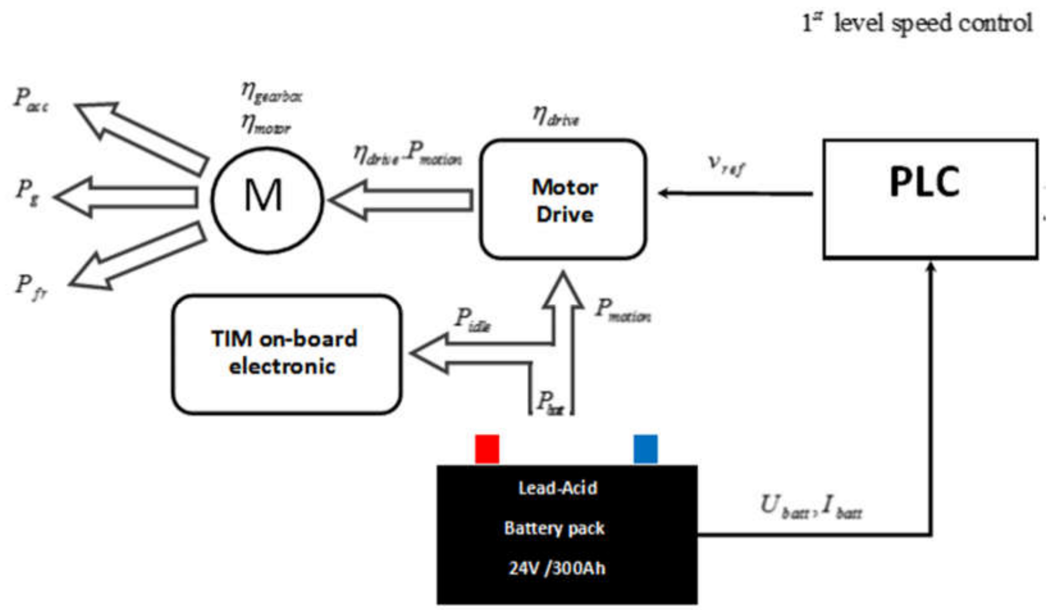

Figure 16: 1st level of TIM speed control and power repartition

The Figure 16 gives an overview of how TIM speed is controlled. Since the PLC provides the speed reference to the motor drive, the evolution of this reference results in a response of current. The model thus have as main input (among other) the speed reference and as an output, the power consumption from which the current will be deduced knowing the battery voltage.

5.1 Acquisition of mission data

Since the model is based on real measurement data and not on analytical formulation, first thing that has been done, is a system which allows to record the measurements needed to establish the current consumption model.

The values available and logged during mission are:

Timestamp :	*Time at which the sample of the set of variable is performed*
I_{batt} :	*Current taken from the battery*
U_{batt} :	*Voltage of the battery*
v :	*Instantaneous velocity of TIM*
DCUM :	*Relative position of TIM in the tunnel wrt origin*

It has been possible the log those data by implementing a LabVIEW VI which recover the values of the above mentioned measured by reading the values published by the OPC server of the PLC on TIM internal network. Indeed, an IPC is installed on the reconnaissance wagon of the train and have access to all the variables published by the different PLCs controlling the train operation. This structure is shown on Figure 17 .

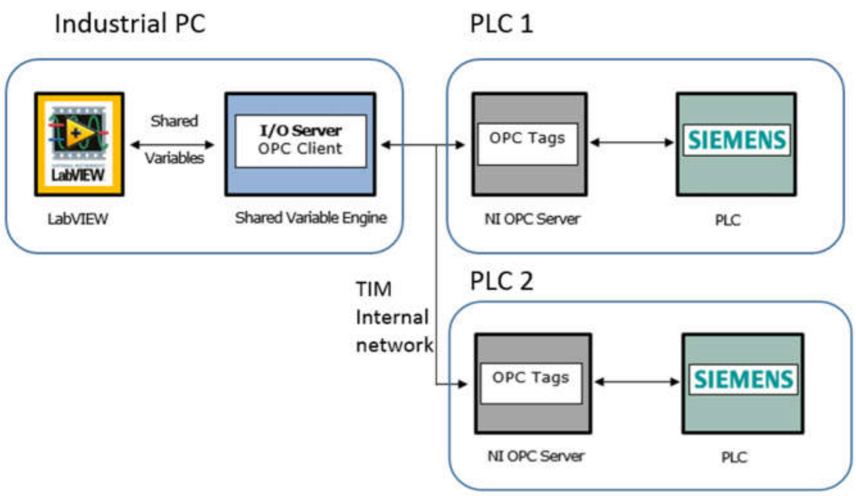

Figure 17: OPC client/server structure

The LabVEW VI that has been implemented on the IPC is retrieving the values of the different measurement and loggs them every 100ms in a text file which can be downloaded at the end of the mission.

A set of data acquired by this mechanism is shown on Figure 18. These data will be used during all the developments of the TIM model.

The reader will notice the presence of a graphic representing the SOC of the battery. These data are provided by the embedded Hoppecke sensor which will be replaced by the SOC estimator presented in Section 2 since this sensor provide overestimated values of the SOC which could lead to fully drained batteries in the middle of a mission.

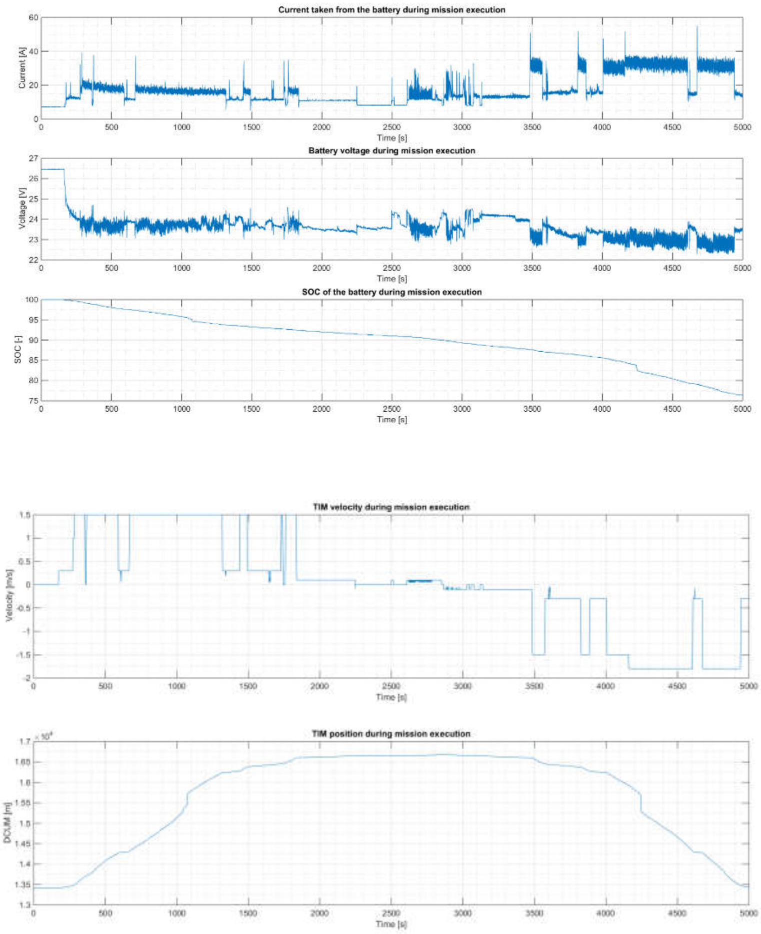

Figure 18: Set of Data acquired during a mission

5.2 TIM power balance

The current consumption model of TIM is based on the global power balance. Since the power consumption can be decomposed into several distinct parts. The idea of this process is to clearly identify the well-known parts and to deduce the unknowns by solving a simple equation.

The overall power consumption of TIM is the summation of the following individual powers (c.f. Figure 16):

$$P_{batt} = P_{Idle} + \frac{1}{\eta_{tot}}\left(P_g + P_{fr} + P_{acc}\right)$$

$$\begin{aligned}
&\textit{with}:\\
&\quad P_{batt}: \text{Total electrical } \textit{power provided by the battery}\\
&\quad P_{Idle}: \textit{ Power needed to feed electronic devices } (\textit{consumption in idle state})\\
&\quad P_{g}\;: \textit{Power needed to compensate earth gravity } (\textit{depends on rail's slope})\\
&\quad P_{fr}\;: \textit{Power needed to compensate friction on rail } (\textit{air resistance assumed null})\\
&\quad P_{acc}: \textit{Power needed to accelerate TIM } (\textit{null at constant speed})\\
&\quad \eta_{tot} = \eta_m . \eta_g: \textit{ global efficientcy of traction chain } \quad (\eta_m = 0.9,\ \eta_g = 0.7)
\end{aligned}$$

Most of these individual powers can be easily identified and formulated but it has not been possible to find a satisfying analytical formulation for the power dissipated by friction. That is why an identification based on real data acquired during the TIM operation has been used.

5.3 The formulation of well-known powers.

As seen in the previous section, the power extracted from the battery is expressed as the sum of several distinct "power consumers". This part will describe the formulation of those which can be formulated using mechanical laws.

5.3.1 Power needed to balance gravity

F_g is the force of earth attraction projected on the axis collinear to the monorail (Figure 19) according to Newton's first law.

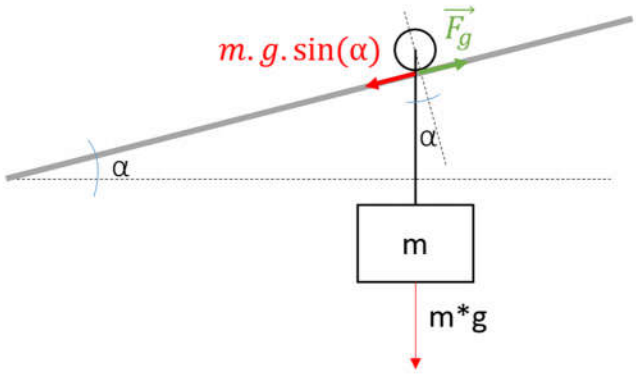

Figure 19: Static equilibrium between earth attraction force and force applied on the rail by the wheel

Then the power needed to balance gravity is equal to F_g multiplied by the train velocity v :

It can be expressed as:

$$P_g = v.\mathrm{m}.g.\sin(\alpha(\mathrm{x}))\ [W]$$

with :

- v : TIM velocity $[ms^{-1}]$
- m : TIM's mass (600kg)
- g: acceleration of gravity $[ms^{-2}]$
- $\alpha(\mathrm{x})$: is the slope of the rail at position x in the tunnel $[rad]$
- x : TIM relative position in the tunnel

5.3.2 Power needed to accelerate the train

Since the train needs to be accelerate/decelerated during its operation, the force applied during these phases is expressed by the Newton's second law:

$$F_{acc} = m.\frac{dv}{dt}\ [\mathrm{N}]$$

Then, P_{acc} is the power necessary to accelerate the train. This power is zero at constant speed.

It can be expressed as:

$$P_{acc} = v.\mathrm{m}.\frac{dv}{dt}\ [W]$$

Reader will notice that this formulation will require at least two samples (to compute the derivative) when going into discrete time domain.

5.3.3 Power needed to supply on-board electronic devices

P_{idle} is the constant power consumption of TIM used to supply PLC, IPC and sensors embedded on TIM. This power is assumed constant even if it can vary a little (approx. +/-5%) bit depending on action performed by the IPC.

It can be expressed as:

$$\begin{cases} P_{idle} = I_{idle}.U_{bat} \\ with: \\ I_{idle} \simeq 7.5A \\ U_{bat} \simeq 24V \\ \Rightarrow P_{idle} \simeq 180W \end{cases}$$

5.4 Friction losses characteristic determination

The only unknown remaining in the power balance of the TIM, is the characterization of the power dissipated by friction w.r.t. train speed. In order to determine this characteristic, it has been decided to proceed as following: Based on the data acquired during a mission, it is possible, knowing the position, the slope of the rail w.r.t. position in the tunnel (Figure 20), the speed of the train, the mass of the train and the global efficiency of the transmission, to compute the contributions of P_{Idle}, P_g and P_{acc} to P_{batt}.

By performing the computations of these contributions on the overall mission duration, the profile of the power dissipated by friction can be found with:

$$P_{fr} = \eta_{tot}\ (P_{batt} - P_{Idle}) - P_g - P_{acc}$$

This method, when applied to the data acquired during a mission, gives the results shown on Figure 21.

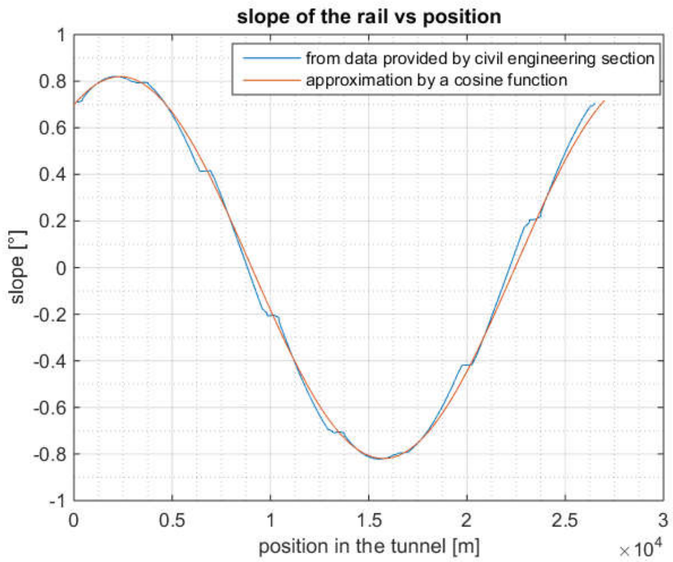

Figure 20: Slope of the rail vs position

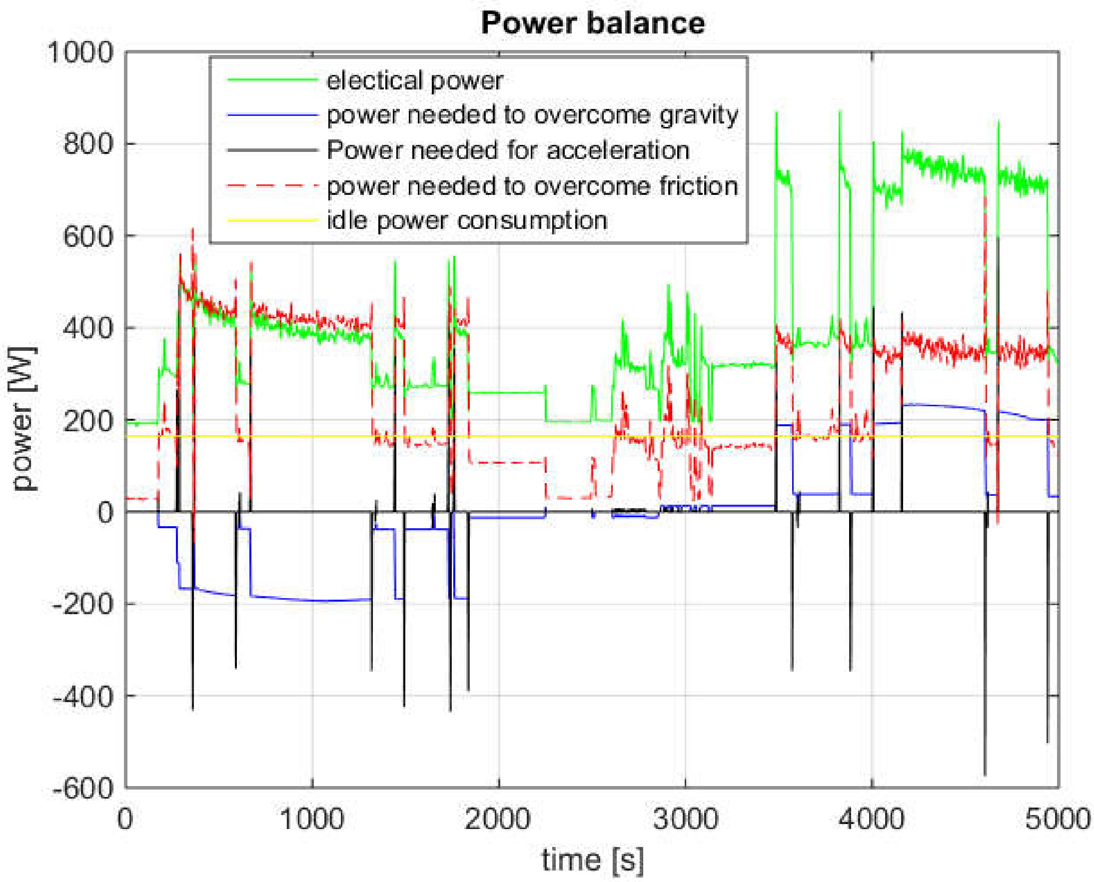

Figure 21: Individual power contribution along mission duration

In order to build the characteristic of the friction losses w.r.t. to the speed, only values obtained when TIM is traveling at a constant speed are considered. This means that measurements during transient phases of acceleration/deceleration are not taken into account. To do so, the profile of P_{fr} goes through a kind of filter that select the values of losses only when the derivative of the speed is null. The values obtained are sorted by speed and averaged. This leads to the curve visible on Figure 22.

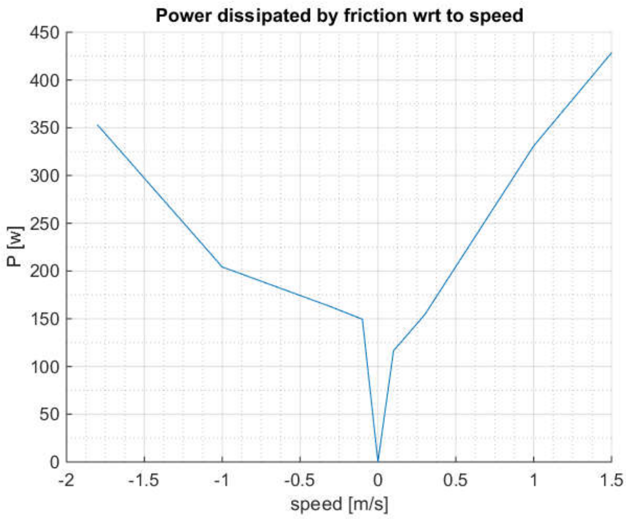

Figure 22: $P_{fr}(\mathrm{v})$, friction losses w.r.t. TIM velocity

The characteristic obtained, is not symmetric. It is suspected that this shape is induced by the tensioning mechanism used to maintain the pressure of the motor wheel on rail, which is not symmetric (Figure 23) and could induce this behavior when absorbing irregularities of the rail. It has been confirmed that the rail, which was originally used to carry the electromagnet in the tunnel, present significant aging signs and irregularities are quite significant (bumps on the surface of contact with the wheels at several position in the tunnel).

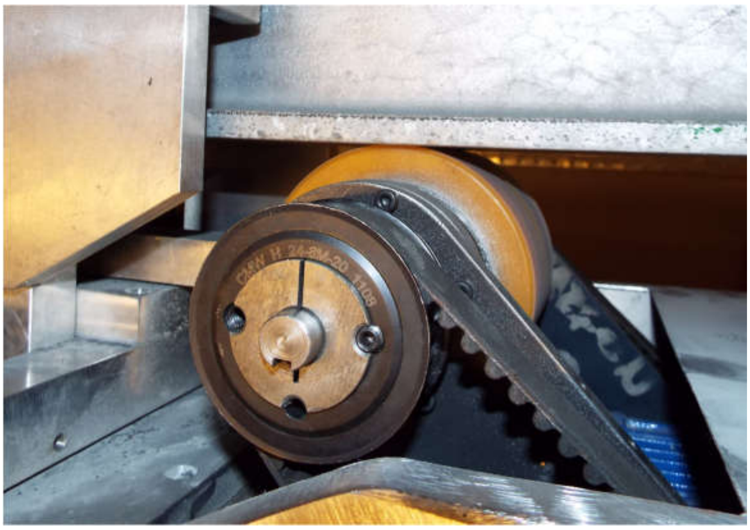

Figure 23: Tensioning mechanism ensuring motricity

The characteristic $P_{fr}(\mathrm{v})$ will be used, in the final model, as a look-up table which takes the speed of the train as an input and return the corresponding value of power dissipated by friction.

5.6 Global TIM power balance model

The global model is obtained simply by combining the individual power consumptions P_{Idle}, P_g, P_{acc} and P_{fr}, considering the efficiency of the traction chain of the train as previously formulated:

$$P_{batt} = P_{Idle} + \frac{1}{\eta_{tot}}\left(P_g + P_{fr} + P_{acc}\right).$$

The complete discrete time formulation can be expressed as following:

$$\begin{aligned}
&P_{batt}[k] = P_{Idle}[k] + \frac{1}{\eta_{tot}}\left(P_g[k] + P_{fr}[k] + P_{acc}[k]\right)\\
&with:\\
&\quad P_{Idle}[k] = P_{Idle} = 180\text{W is a constant}\\
&\quad P_g[k] = v[k].m.g.\sin(\alpha(\mathrm{x}[k]))\\
&\quad P_{acc}[k] = v[k].m.\frac{[v[k] + v[k-1]]}{\Delta t}\\
&\quad P_{fr}[k] = f(v[k]) \ \text{:power returned by the lookup table}\\
&and\ where:\\
&\quad \Delta t:\ is\ the\ sampling\ period\\
&\quad k:\ is\ the\ sample\ index
\end{aligned}$$

This formulation has been implemented according to the functional diagram shown on Figure 24.

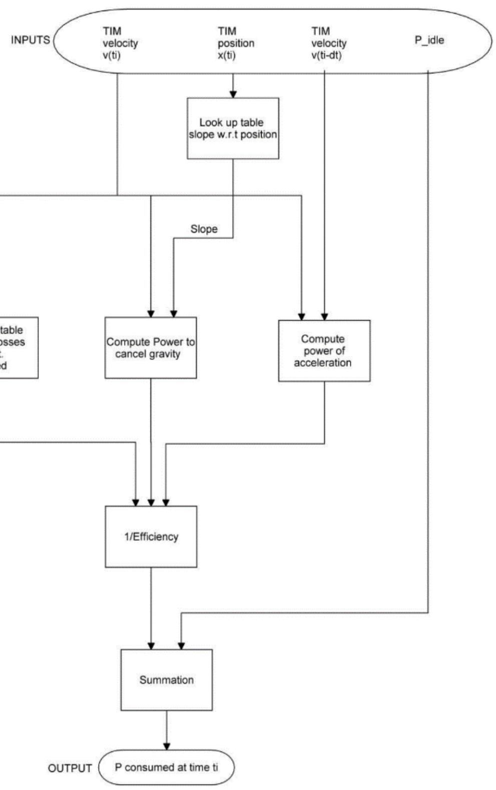

Figure 24: Functional diagram of the model

5.7 Result of the TIM power consumption model

In the insight of forecasting the energy required to perform a mission with the TIM, the model has to be proven accurate enough before being used. Also, always considering the same set of data, the model has been tested as follow:

1- The mission speed profile and position is given as an input to the model.
2- The model returns the power profile for the whole mission duration.
3- From Power profile is deduced the current consumption profile (for $U_{batt} = 24V$)
4- From the current consumption profile is deduced the SOC evolution over mission duration

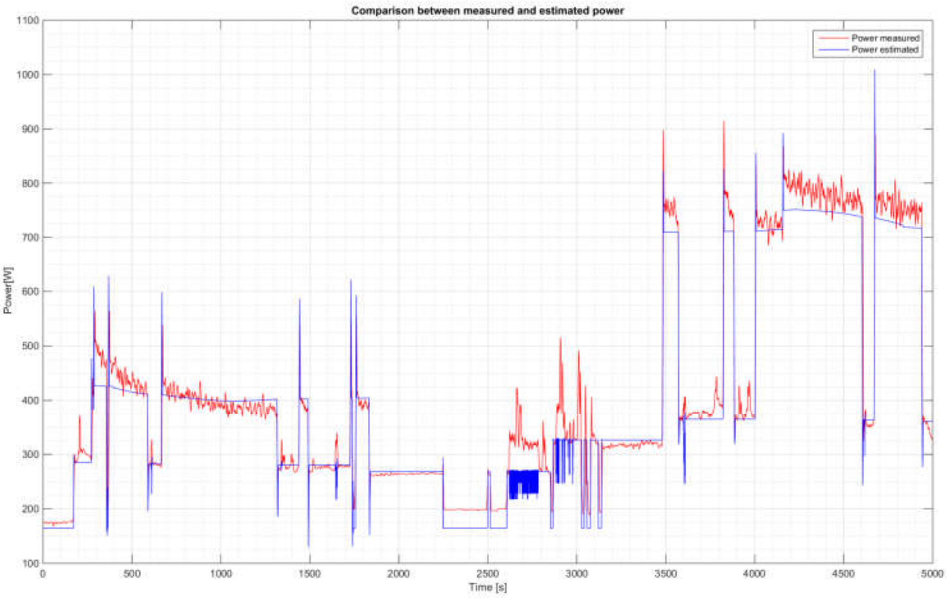

Figure 25: Real and estimated power profiles

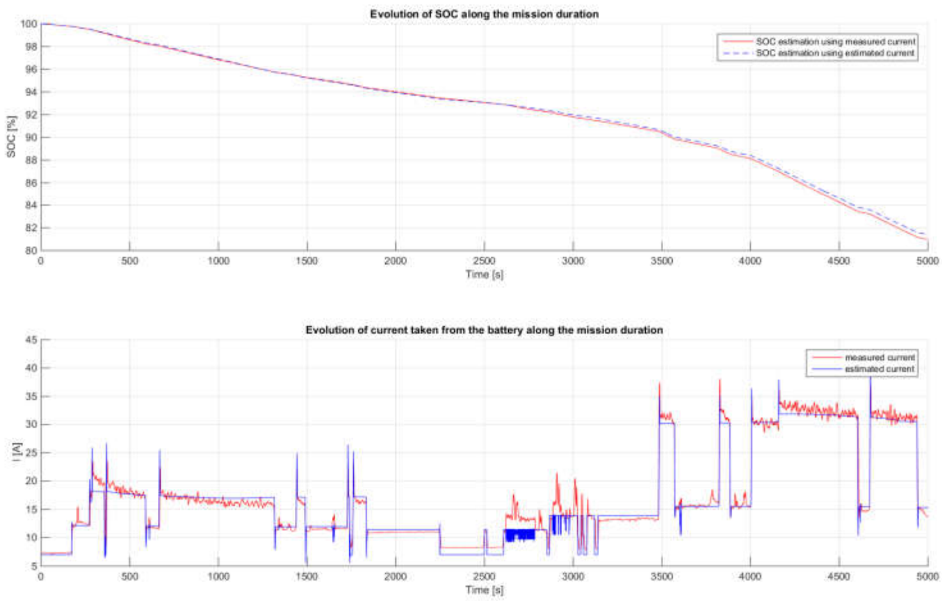

Figure 26: Real and estimated SOC and Current profiles

Steps 1 and 2 lead to the results shown on Figure 25. It can be stated that the predicted power consumption sticks pretty well to the actually power actually consumed by the train even if little deviations can be seen on several period of the mission, especially between t=2600s and t=3000s. It can be thought that some perturbation or external force intervene during this period since these perturbation are visible on raw data of Figure 18, that the velocity also presents these perturbations when it should be constant on this interval (0.1m/s).

The interpretation of these results is only qualitative still the model seems to provide satisfying results, since when having a look at the comparison between SOC computed with the real current and the one with estimated current profile found by applying steps 3 and 4, first give a final value of 80.98% and second gives 80.77%. This means that the absolute error value is only 0.21% and relative one is 0.00259% for a discharge duration of 1 hour and 20 min.

Further tests will be performed with other measurement when those will be available but it is already possible to state that the model reflect quite well the TIM power consumption. Moreover, given a defined speed profile, start position of a mission, it is possible to determine with a relatively high accuracy, the final SOC at the end of the mission.

6 Energy consumption optimization

When dealing with electrically powered vehicles and more generally in every power consuming system, it is always interesting to minimize the energy required for the operation of the system. The minimization can be achieved in several ways.

First way to make a system energetically efficient, is to minimize intrinsic losses of the system. This can be done by paying attention during the development phase to only use energetically efficient sub-systems (it can be electronic devices or mechanical system or anything inducing losses). Second way to minimize losses, is to pay attention on how the energy is used and to do not an irrational use of it.

An obvious example of this second way to minimize energy consumption can be given by the case of a car driver, driving on a road with a traffic light ahead. It is obvious that this driver does not have interest, if he wants to save gasoline, to floor the accelerator if he has seen that a traffic light is red 50m behind. The natural and energy friendly behavior would be to maintain a constant speed until the distance with the obstacle is judged short enough to let the car decelerate gently, to do not have to dissipate too much energy in the brakes. By adopting this behavior, the driver can extend the number of kilometers he will be able to travel with the amount of fuel remaining in the tank of the car and moreover reduce the cost or his trip. This behavior is possible only if the driver of the system knows what is going to happen in the future. It means that this an energy-friendly behavior is based on predictions.

Since, in the case of TIM system, it is not thinkable to modify drastically its design and in order to try to save energy to extend the autonomy, the second way to be envisaged in order to save the energy stored in the batteries.

The purpose of this section is to attempt to develop a speed controller, knowing the characteristics of a mission, able to determine which speed is the most adapted to its current state in order to minimize the energy consumption.

6.1 TIM 1st and 2nd level speed management

TIM is moving along a monorail attached to the ceiling of the tunnel of the LHC. In order to preserve the mechanic and to ensure the security of its operation, the velocity of the train is limited by software depending on the position in the tunnel. Indeed, because of the curve of the rail or due to obstacles present in the tunnel, the speed is limited in some areas (see Table 4). This data are stored in the PLC embedded on TIM and knowing train position, the PLC prevents train from going over the speed limits.

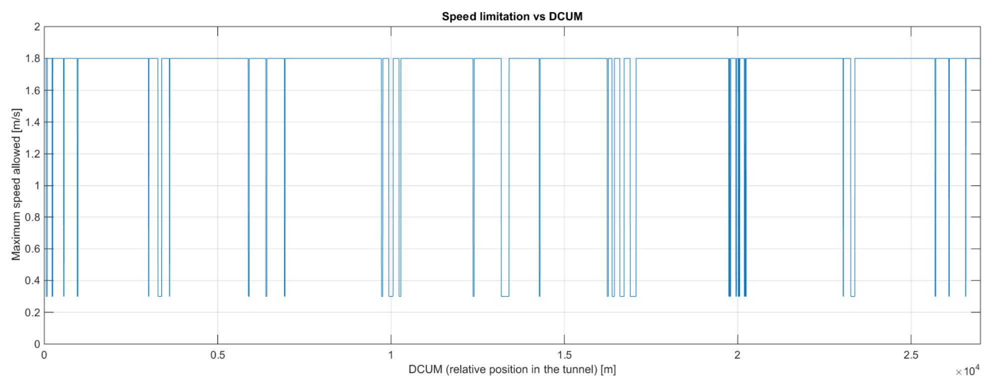

Figure 27: Speed limitations vs position

Obstacle	Type	DCUM1 [m]	DCUM2 [m]	COMMENT	Retract RP arm?	Max speed allowed [m/s]
UJ17	Chicane	55	85	Not-possible-to-pass	T	0
RR17	Chicane	223	243		T	0.3
RT18	Chicane	558	568		T	0.3
R19	Sector-door	949	969	YCPS01-dcum-959	T	0.3
UJ22	Chicane	3005	3015	YCPS01-dcum-3010-red-door	T	0.3
UJ24-UJ26	Shielding	3279	3385	Not-possible-to-pass	T	0
UJ27	Chicane	3609	3619		T	0.3
UJ32	Ventilation-door	5883	5907	dcum-5897	T	0.3
R34	Sector-door	6390	6420	YCPS01-dcum-6399.5	T	0.3
R37	Sector-door	6925	6945	YCPS01-dcum-6935.6	T	0.3
RA43	Sector-door	9725	9763	YCPS01-dcum-9753	T	0.3
UJ44-UJ46	Chicanes	9936	10060	very-close-to-wall	T	0.3
RA47-UJ47	Sector-door	10232	10283	YCPS01-dcum-10241.9	T	0.3
R51	Sector-door	12365	12400	YCPS01-dcum-12381.9	T	0.3
UJ53-UJ56	Chicanes	13180	13405	Bypass-P5	F	0.3
R59	Sector-door	14275	14299	YCPS01-dcum-14288.2	T	0.3
UJ62	Chicanes	16236	16267		T	0.3
UJ63-RA63	Chicane + door	16375	16441	YCPS01-dcum-16430	T	0.3
UJ64-UJ66	Chicanes	16600	16722		T	0.3
RA67-UJ68	Sector-door	16900	17067	YCPS01-dcum-16905.5	T	0.3
R74	Sector-door	19740	19760	YCPS01-dcum-19753	T	0.3
R74	Ventilation-door	19777	19797	YCPV02-dcum-19788	F	0.3
R74	Ventilation-door	19945	19965	YCPV01-dcum-19955	F	0.3
UJ76/R76	Ventilation-door	20017	20032	YCPV01-dcum-20024.5	T	0.3
R771	Ventilation-door	20039	20059	YCPV01-dcum-20049	F	0.3
R771	Ventilation-door	20190	20210	YCPV02-dcum-20200	F	0.3
R771	Sector-door	20225	20245	YCPS01-dcum-20235	T	0.3
UJ83	Chicane	23039	23049		T	0.3
UJ84-UJ86	Shielding	23260	23378	Not-possible-to-pass	T	0.3
R11	Sector-door	25691	25711	YCPS01-dcum-25701	T	0.3
RT12	Chicane	26091	26101	ATLAS-bypass	T	0.3
UJ13	Chicane	26572	26582		T	0.3
UJ13	Shielding	26603	0	Not-possible-to-pass	T	0

Table 4: List of obstacles in the LHC tunnel with corresponding speed limitations

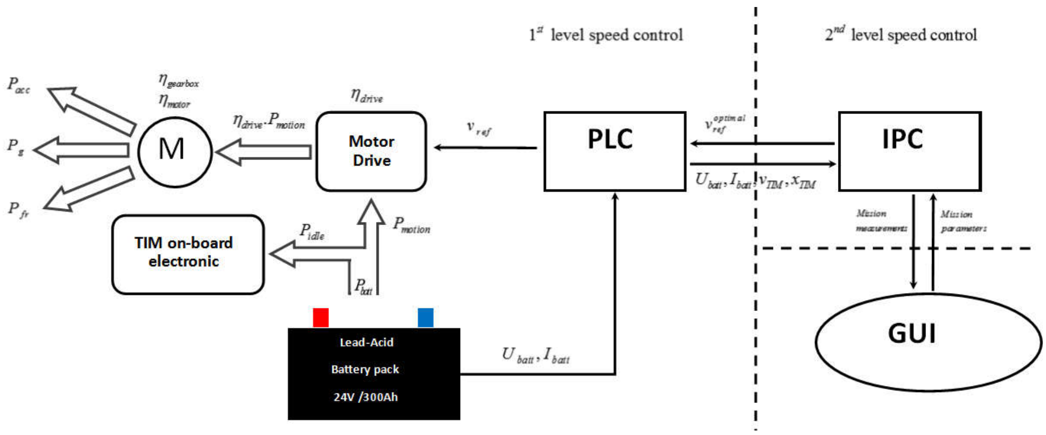

Figure 28: TIM Speed control levels 1 and 2

The second level is the one actually giving the speed reference to TIM. This reference is bound by the 1st level in order to limit the maximum speed. It is at the 2nd level that the optimization will provide the speed reference to send the most adapted speed in order to minimize energy consumption. A representation of the architecture of the speed control of TIM can be seen on Figure 28. It highlights that the 2nd level speed reference can be provided either directly from the IPC or from the remote GUI. Since the train must act in a standalone way, the optimized speed has to be provided by the IPC embedded on TIM. The consequences is that the optimization must run on this latter.

6.2 Optimization principle

Once the operator has configured the mission he wants to perform, the parameters of the mission are sent to the IPC. At this stage, all the information required for the mission are stored on-board and TIM can perform the mission even if a loss of communication occurs. This means that, among other, the start point, the destination and eventually the 2nd destination are known. These values are mandatory to launch the optimization since, it will be explained later that this latter is based on the knowledge of the path TIM has to travel in order to determine the most adapted speed to minimize energy consumption. The data shown on Figure 27 are stored on the computer in charge of the optimization. With these data, the algorithm extract the region corresponding to mission start and end points. This allows it to get the information about the maximum speed profile TIM can perform along the mission path.

The formulation of the optimization is aiming at two main goals:

-First, it must minimize as much as possible the energy spent on a determined mission without impacting too much the duration of the mission.

-Second, it must respect the operation limit of the TIM (for instance, in must not exceed maximum current that the battery can provide, the maximum power, the minimal voltage between battery leads, etc.).

This are the two key points, first will define the objective function and second will determine the constraints of the optimization problem.

6.3 Choice of the decision variable

In order to formulate the optimization problem, the choice of the decision variable must be done carefully. Indeed, in order to keep a reasonable number of equations, this choice is crucial in order to keep the problem solvable by the machine it is running on. Also, the path of the mission will be discretised and decision variable will correspond to the speed at each discretised location. This allows to have a control on the length of the decision variable vector and consequently on the number of equations to solve.

The decision variable is defined as:

$$X = \begin{bmatrix} v_1 \\ v_2 \\ . \\ v_i \\ . \\ v_N \end{bmatrix} \text{ with i an integer within } [1\ ;\ N]$$

Each element of X is a speed reference linked to the mission position sample i.

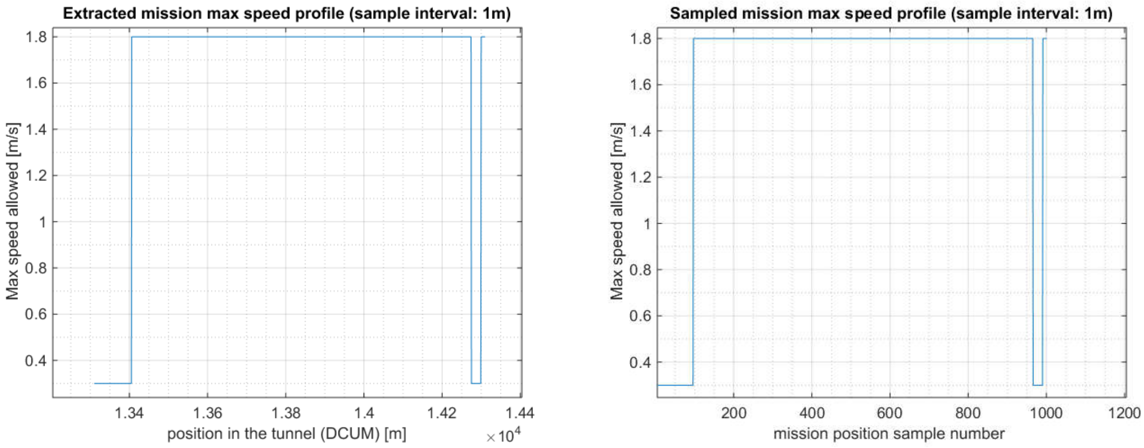

Figure 29: Extracted mission path (left) sampled mission path (right) for a 1000 meter long mission

The discretization interval of the path of the mission has been chosen to be 1m. This will prevent the optimized speed reference to be bounded by the 1st level of the speed control. Indeed, the PLC consider that TIM must slow down 10m before entering an area where the speed limitation change. In order to does not let the PLC limit the speed reference, this distance will be increased to 11m in the data considered by the optimization problem.

6.4 Definition of the objective function

The objective or cost function is the one to be minimized. Indeed, in the case of TIM, the objectives are double: minimize mission duration and energy spent during the mission.

This can be formulated as following:

$$\text{obj} = \min_{v_i} \sum_{i=0}^{N} \alpha(\text{v}_{\max,i} - v_i)^2 + \beta(\Delta\text{SOC}_i)^2$$

with:

- $\text{v}_{\max,i}$: maximum speed allowed at sample i of the mission path
- v_i : element i of the decision variable X
- ΔSOC_i : Variation of the SOC corresponding to v_i over sampled mission path interval i and i+1
- α : weight of mission duration minimization
- β : weight of energy consumption minimization

Following this formulation, the problem aims at finding the best value of the elements v_i of the decision variable X in order to minimize the mission duration and the energy consumption.

6.5 Definition of the constraints

6.5.1 Inequality constraint on positive acceleration

The constraint on positive acceleration corresponds to the train maximal acceleration $a_{\max,i}$. This value is equals to 0.45 m.s^{-2} (value limited by the PLC speed management)

Constraint on positive acceleration can be expressed as:

$$v_i - v_{i-1} \leq a_{\max,i} \qquad \text{(a)}$$

6.5.2 Inequality constraint on negative acceleration (deceleration)

Similarly to the positive acceleration limit, the value of $a_{\min,i}$ is equals to -0.45 m.s^{-2}.

Constraint on deceleration can be expressed as:

$$v_{i-1} - v_i \geq a_{\max,\mathrm{i}} \qquad \text{(b)}$$

6.5.3 Inequality constraint on maximum speed

Constraint on the maximum speed is given by the maximum speed profile value at index i. This constraint will prevent TIM from over-speeding, depending if it is in an obstacle area or not (0. or 1.8 ms^{-1})

Constraint on maximum speed can be expressed as:

$$v_i \geq v_{\min,i} \qquad \text{(c)}$$

6.5.1 Inequality constraint on minimum speed

Similarly to maximum speed constraint, this one corresponds to the negative value of the speed limits (when the train is going in the opposite direction).

Constraint on minimum speed can be expressed as:

$$v_i \leq v_{\max,i} \qquad \text{(d)}$$

6.5.2 Inequality constraint on maximum power consumption

The constraint on maximum power consumption is supposed to add a limitation on maximum power that can be taken from the battery. The real value of this limit is 10.8kW. But in this case, the battery is discharged in less than 100s. Thus, this limit has been set to 2kW since 1.5kW is the maximum power ever measured on TIM. This allows a little power margin.

Constraint on maximum power consumption can be expressed as:

$$U_i^{batt}.\mathrm{I}_i^{batt} \leq P_{\max}^{batt} \qquad \text{(e)}$$

6.5.3 Inequality constraint on maximum current consumption

Similarly to constraint on maximum power consumption, the maximal current deliverable by the battery is 450A. The maximum current ever measured is around 70A so this value has been taken as a limit for $\mathrm{I}_{\max}^{batt}$.

Constraint on maximum current can be expressed as:

$$\mathrm{I}_i^{batt} \leq \mathrm{I}_{\max}^{batt} \qquad \text{(f)}$$

6.5.4 Inequality constraint on minimal voltage

The constraint on minimal voltage is set to be equals to EODV in order to prevent damages that could occur when the battery is brought below this limit. For one battery the EODV is 10V, thus 20V is taken for $U_{\max}^{batt}$

Constraint on minimum voltage can be expressed as:

$$U_i^{batt} \geq U_{\min}^{batt} \qquad \text{(g)}$$

6.5.5 Non-linear Constraint on SOC evolution

This constraint only prevents SOC from being lower than the minimal SOC_{min}. It value has arbitrary been set to 30%.

$$SOC_N \geq SOC_{\min} \qquad \text{(NL inequality constraint)} \qquad \text{(h)}$$

6.5.6 Equality constraint on Battery voltage

This constraint is supposed to reflect the evolution of the battery voltage depending on the internal impedance of the battery and on the current it provides. Unfortunately, the tests allowing the determination of R_{eq} have not been performed due to lack of time. This constraint will remain will the average value of the battery voltage observed during missions where measurement have been made. The average value of the voltage is $U_i^{batt} = 23.5$V.

$$U_i^{batt} = U_O - R_{eq} I_i^{batt} \qquad \text{(i)}$$

6.5.7 Equality constraint on power consumption

$$U_i^{batt}.\mathrm{I}_i^{batt} = I_{idle} U_i^{batt} + \frac{1}{\eta}\left(m.g.v_i.\sin(\alpha) + g(v_i) + \left[P_{acc}\right]\right) \qquad \text{(j)}$$

6.5.8 Equality constraint on SOC

$$SOC_i = SOC_{i-1} + \frac{I_i^{batt}}{C(\mathrm{I},\theta)}.\frac{\Delta x}{v_i} \qquad \text{(NL equality constraint)} \qquad \text{(k)}$$

6.6 Global problem

The total problem formulation is simply obtained by gathering all the above equations. This problem has been implemented only partially on Matlab since equality constraint (i) has been replaced by $U_i^{batt} = 23.5\text{V}$. This means that the battery voltage is considered constant and non dependant on SOC and current. using the fmincon function which allows to solve non-linear optimization problems.

$$\min_{v_i} \sum_{i=0}^{N} (\text{v}_{\max,i} - \text{v}_i)^2 \qquad \text{(O)}$$

$$\textit{Subject to}:$$

$$v_i - v_{i-1} \le a_{\max,i} \qquad \text{(a)}$$

$$v_{i-1} - v_i \ge a_{\max,\text{i}} \qquad \text{(b)}$$

$$v_i \ge v_{\min,i} \qquad \text{(c)}$$

$$v_i \le v_{\max,i} \qquad \text{(d)}$$

$$U_i^{batt}.\text{I}_i^{batt} \le P_{\max}^{batt} \qquad \text{(e)}$$

$$\text{I}_i^{batt} \le \text{I}_{\max}^{batt} \qquad \text{(f)}$$

$$U_i^{batt} \ge U_{\min}^{batt} \qquad \text{(g)}$$

$$SOC_N \ge SOC_{\min} \quad \text{(NL inequality constraint)} \qquad \text{(h)}$$

$$U_i^{batt} = U_O - R_{eq} I_i^{batt} \qquad \text{(i)}$$

$$U_i^{batt}.\text{I}_i^{batt} = I_{idle} U_i^{batt} + \frac{1}{\eta}\left(m.g.v_i.\sin(\alpha) + g(v_i) + \left[P_{acc}\right]\right) \qquad \text{(j)}$$

$$SOC_i \le SOC_{i-1} + \frac{I_i^{batt}}{C(\text{I},\theta)}.\frac{\Delta x}{v_i} \quad \text{(NL inequality constraint)} \qquad \text{(k)}$$

6.7 Implementation in Matlab

The implemented Matlab script can be seen in appendix

Matric form of the decision variable:

$$X = \begin{bmatrix} v_1 \\ v_2 \\ . \\ . \\ v_N \end{bmatrix}$$

Formulation of constraints on accelerations under the matrix form A.x<b (N=4 for readability)

(a) Constraint on positive acceleration can be expressed in matrix form as:

$$A_{acc}X \le b_{acc}$$
with
$$A_{acc} = \begin{bmatrix} -1 & 1 & 0 & 0 \\ 0 & -1 & 1 & 0 \\ 0 & 0 & -1 & 1 \\ 0 & 0 & 0 & 0 \end{bmatrix}$$
$$b_{acc} = 0.1 \left[ms^{-2} \right]$$

(b) Constraint on negative acceleration is expressed in matrix form as:

$$-A_{acc}X \ge b_{acc}$$

Merging (a) and (b) leads to:

$$A_{acc}^{tot}X \le b_{acc}$$
with
$$A_{acc}^{tot} = \begin{bmatrix} A_{acc} \\ \cdots \\ -A_{acc} \end{bmatrix} = \begin{bmatrix} -1 & 1 & 0 & 0 \\ 0 & -1 & 1 & 0 \\ 0 & 0 & -1 & 1 \\ 1 & -1 & 0 & 0 \\ 0 & 1 & -1 & 0 \\ 0 & 0 & 1 & -1 \end{bmatrix}$$
$$b_{acc} = 0.1 \left[ms^{-2} \right]$$

(c) Constraint on maximum speed can be expressed in matrix form as:

$$I_N . \mathrm{X} \le \left[v_{\max,i} \right]$$
with
$$I_{N=4} = \begin{bmatrix} 1 & 0 & 0 & 0 \\ 0 & 1 & 0 & 0 \\ 0 & 0 & 1 & 0 \\ 0 & 0 & 0 & 1 \end{bmatrix}$$

$v_{\max,i}$ are derived from maximum speed allowed at corresponding positions

(d) Constraint on minimum speed can be expressed in matrix form as:

$$I_N . \mathrm{X} \ge \left[v_{\min,i} \right]$$

$v_{\min,i}$ are derived from maximum speed allowed at corresponding positions

(e) Constraint on maximum power consumption can be expressed in matrix form as: (neglecting Pacc)

$$A_{power}.\mathrm{X} \leq \mathrm{P}_{\max}^{batt} - P_{idle}$$
$$A_{power} = diag(h(\mathrm{x}_1), h(\mathrm{x}_2), ..., h(\mathrm{x}_N))$$
with :
$$h(\mathrm{x}_i) = \frac{1}{\eta}\left(m.g.\sin(0.0143\cos(\frac{2.\mathrm{pi}}{26800}\mathrm{x}_i - 0.55)) + 520/1.8 \right)$$

(f) Constraint on maximum current consumption
Never hit, not implemented

(g) Constraint on battery minimum voltage
Not implemented

(h) For now Ubatt = 23.5V

(i) Non-linear inequality Constraint on final SOC

(J) Equality constraint on battery voltage

Ubatt = 23.5V

(K) Equality constraint on power balance

(L) Non-linear relaxed equality constraint on SOC.

6.8 **Results**

The result provided by the implementation in Matlab are not satisfying. Indeed, the values returned are always very close to the maximum speed values regardless of the length the profile or the position of the mission. It is maybe due to a wrong an error or to an excess of simplification in the implementation but another option is to take into consideration:

It could be possible that since the power consumed the electronic of the train is too high (180W) in comparison to the power needed to actuate it (between 300 and 800W). Indeed, in that case, the only way to minimize the decrease of the SOC is to reach as fast as possible the destination in order to limit the impact of this power consumption not dependant on TIM motion.

So far, the best SOC that has been achieved at the end of the simulated mission is the same as the one obtained with the maximum speed profile. This gives no interest to the optimization systeme compared to the actual speed control system installed on TIM.

A special effort will be put on trying to find the reason why the algorithm does not allow to find a speed profile which minimized the decreased of the State of Charge in order to be able to present it during the oral presentation of the thesis.

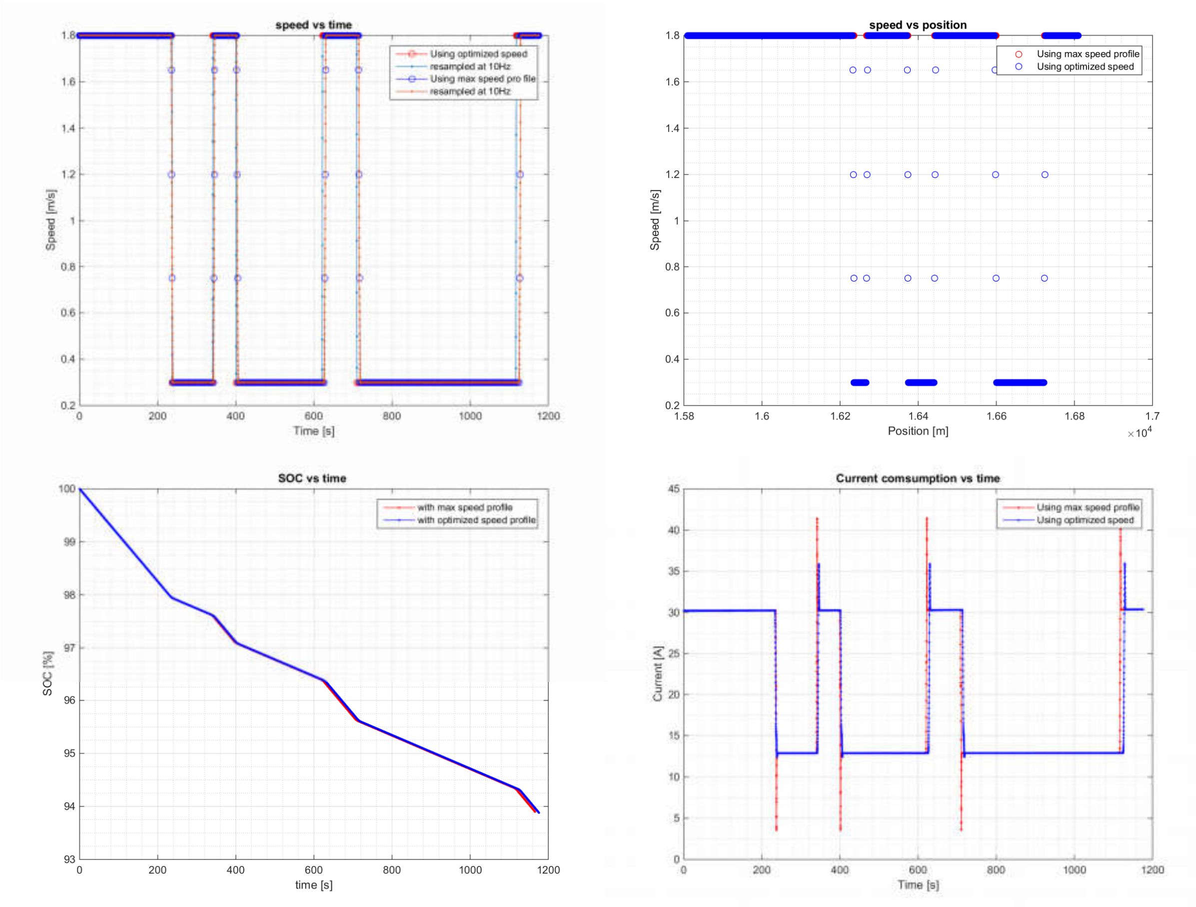

Figure 30: Results of optimization #1

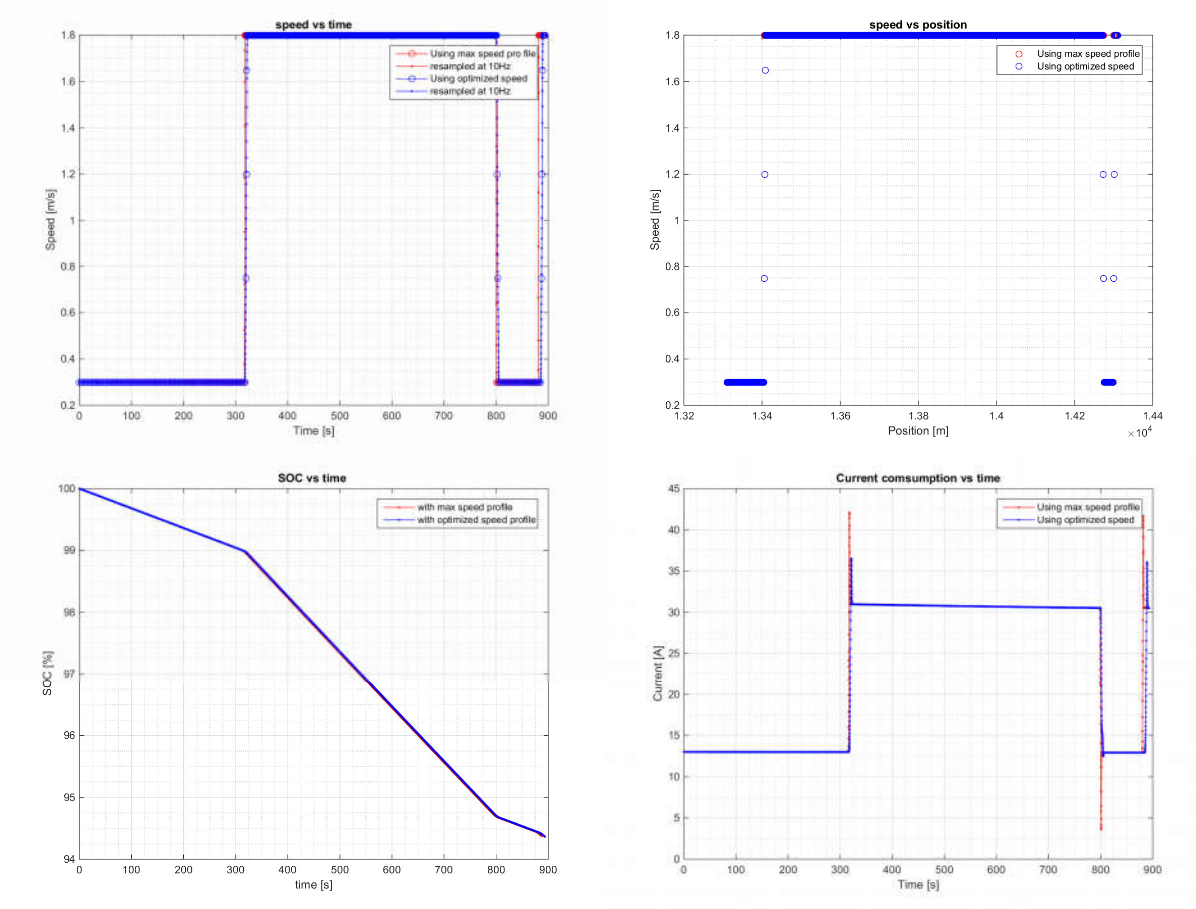

Figure 31: Results optimization #2.

6.9 Results explanations

It could seem weird that the optimization problem always converge to the maximum speed limit but after further tests and research, the reason for this has been found. The curve of $\frac{dSOC}{dx}$ vs speed has been plot and it can be noticed that the faster the train goes, the more efficient it is.

This curve is shown on Figure 32 and clearly shows that this function is monotonously decreasing with speed.

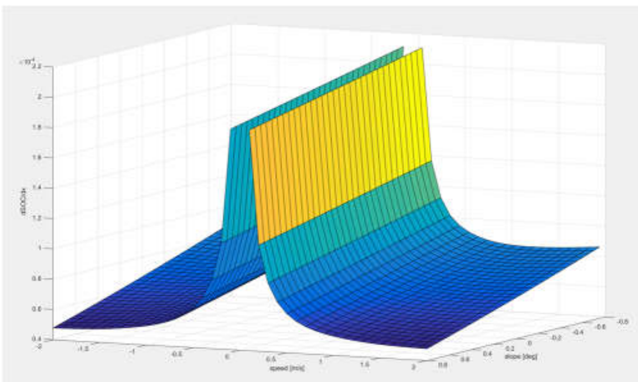

Figure 32: dSOC/dx vs speed and slope

7 Conclusion

This project has reached its first two objectives which are to develop a reliable way to estimate the State-Of-Charge of the batteries ensuring TIM power supply and to estimate the amount of energy needed to perform a mission before launching it. Many improvement are still possible on these two systems and more specifically to the second which has not been incorporated in the TIM system. Indeed the system used to forecast energy consumption stayed at a stage where user has to enter manualy the parameters and run the forecasting manually. One has to keep in mind that TIM system operation is quite complex since it involve a lot of different devices communication between each other but also that the train is actually installed in the tunnel without possibility to access it until next technical stop planned for September. Also during all the period of development of this project, it was rarely possible to move the train to test the implementation since the particles beam was almost always on which does not allow to operate the train.

On the other hand, objectives have not been reached regarding the optimization of the energy consumption. Indeed, results obtained are not satisfying for now since the simulations show that the amount of energy spent is more important when the “optimized speed profile” is applied. A particular effort will be put on this in order to reach the objective before project defense. It has also to be determined if the optimized speed is indeed between operation limits of the train since it could be possible that the best speed profile minimizing the energy consumption is outside the speed range.

Also, despite the fact that all objectives have not been reached, the added value brought to the TIM is real. Indeed, some of the work accomplished is already implemented on the train and some of it will be soon. Also working in such an international environment is a great experience, from cultural point of view but also on the language point of view. Last, even if it was not particularly recommended, several other projects has been developed during last six months. Main one is a complex GUI in LabVIEW able to control robotic Kuka arms placed in the most radioactive area of CERN (ISOLDE plant), requiring a high level of reliability since human intervention in this area is not allowed at all as radioactive material are stored.

To conclude, CERN allows students to perform their internship and master thesis in a very motivating environment, with challenging projects and great specialists. It has been a real honor and chance to participate to the development of such an interesting project as the Train Inspection Monorail, which is in constant evolution and daily improving.

8 Table of figures

9 References

[1] "About CERN," [Online]. Available: http://home.cern/about. [Accessed 25 07 2016].

[2] Bruno Belvedere, Michele Bianchi, Alberto Borghetti, Carlos Alberto Nucci, Fellow IEEE, Mario Paolone, Senior Member IEEE, Antonio Peretto, "A Microcontroller-Based Power Management System for Standalone Microgrids With Hybrid Power Supply," *IEEE transactions on sustainable energy,* vol. 3, no. 3, July 2012.

[3] D. J. Deepti and V. Ramanarayanan, "State of charge of lead acid battery," *India International Conference on Power Electronics, Chennai,,* pp. 89-93., 2006.

[4] Keysight-Technologies, "Application note for battery testing, http://literature.cdn.keysight.com/litweb/pdf/5952-4191.pdf?id=1000000183:epsg:apn," [Online].

[5] X. Wu, D. Freese, A. Cabrera and W. A. Kitch, "http://www.cpp.edu/~wakitch/arts/Wu_et_al_(2015).pdf," 2015. [Online]. [Accessed 13 07 2016].

[6] Y. Qin, B. Zhang and M. Kezunovic, "Optimization of Electric Vehicle Movement for Efficient Energy Consumption," 2014.

10 Appendices

10.1 Results of SOC estimator validation

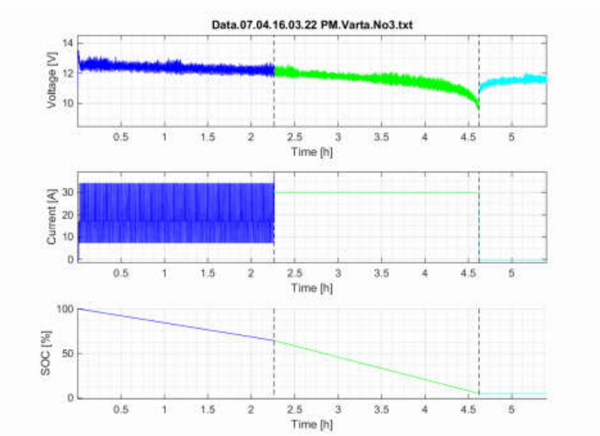

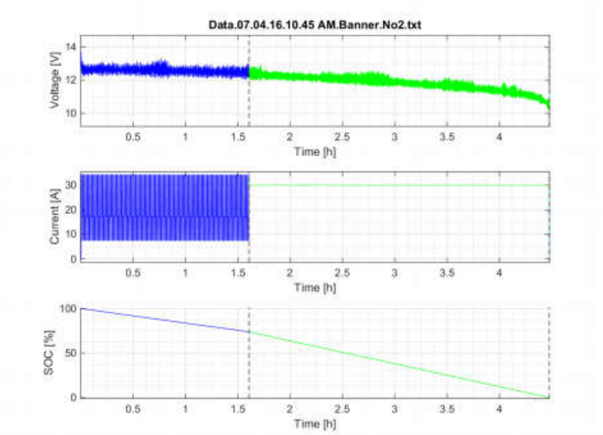

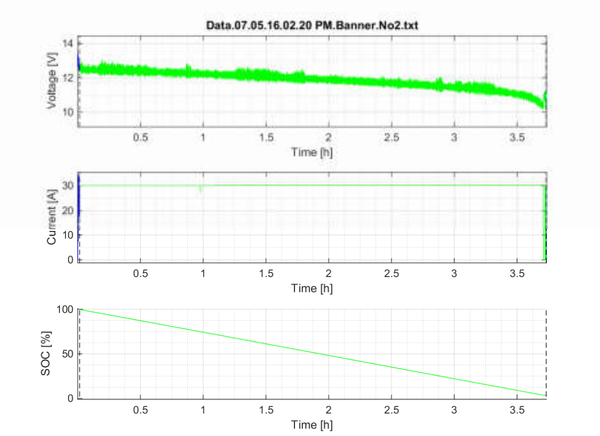

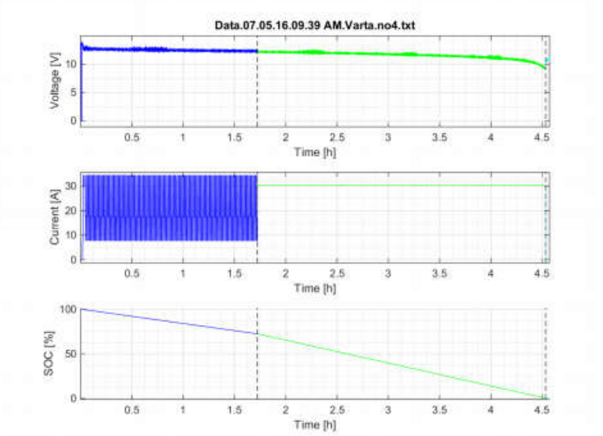

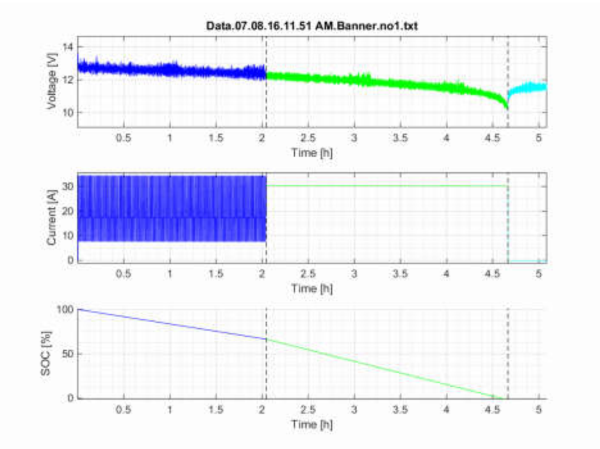

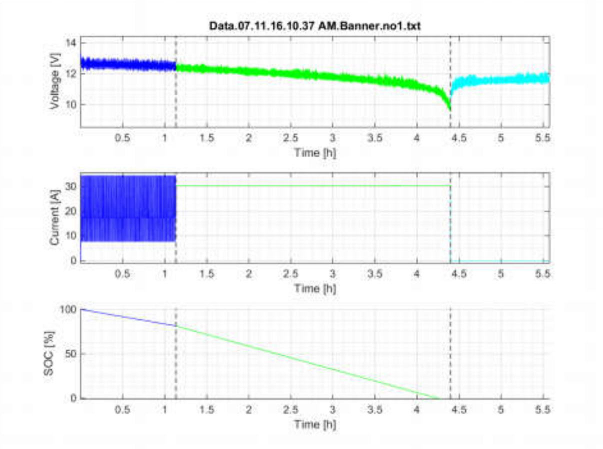

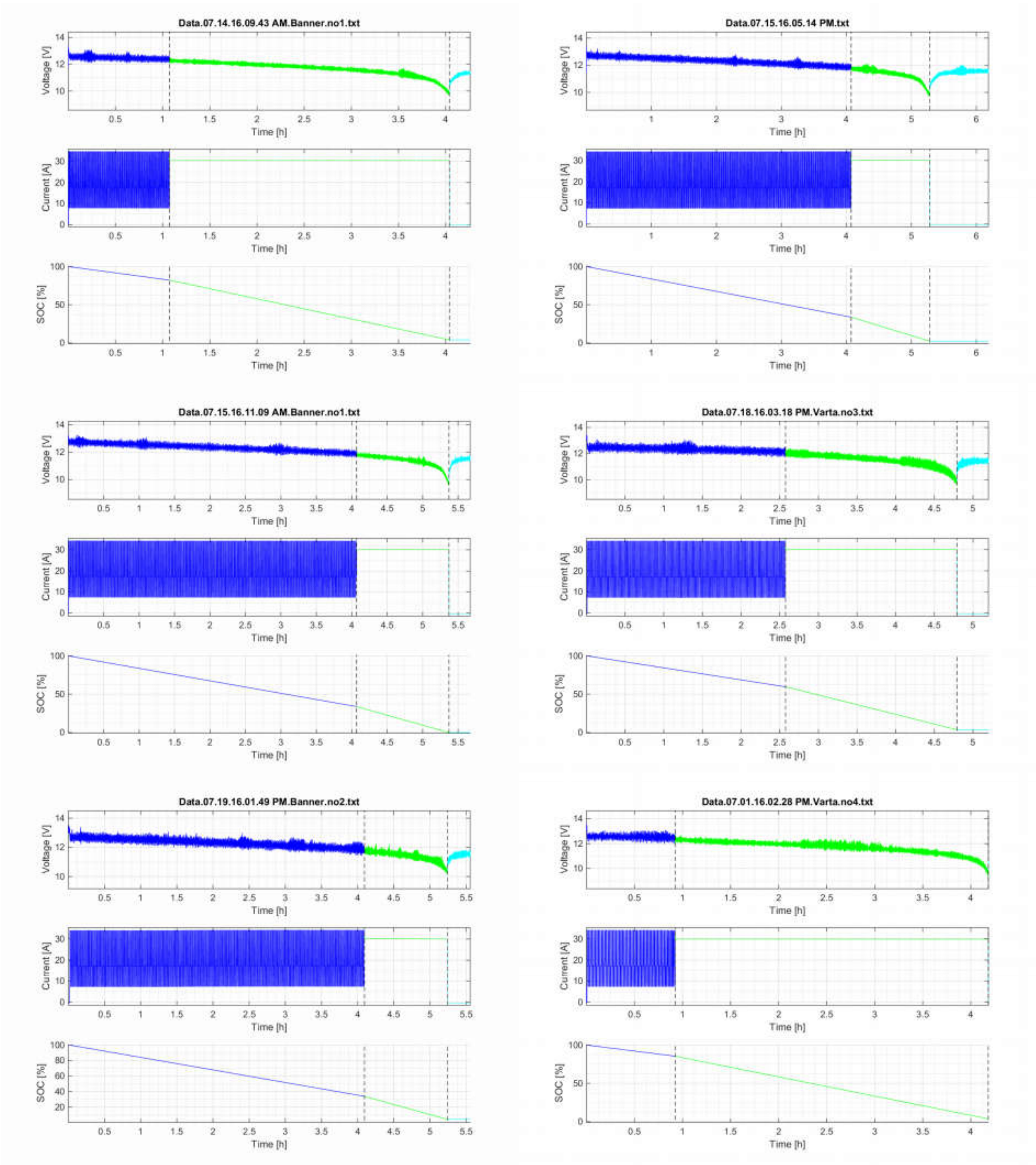
Data.07.14.16.09.43 AM.Banner.no1.txt
Data.07.15.16.05.14 PM.txt
Data.07.15.16.11.09 AM.Banner.no1.txt
Data.07.18.16.03.18 PM.Varta.no3.txt
Data.07.19.16.01.49 PM.Banner.no2.txt
Data.07.01.16.02.28 PM.Varta.no4.txt
Voltage [V]
Current [A]
SOC [%]
Time [h]

<u>Corresponding analysis values:</u>

Varta battery

```
----------------------------------------------------------------------
Data_07_01_16_02_28 PM_Varta_no4.txt
----------------------------------------------------------------------
Total discharge duration: 4.1823 h
Total energy extracted: 115.1576 Ah
Energy extracted during 1st phase: 17.9682 Ah
Energy extracted during 2nd phase: 97.1889 Ah
Depth Of Discharge after 1st phase: 15.6031 %
SOC real after 1st phase: 85.3917 %
SOC estimated after 1st phase: 85.5209 %
SOC estimation error: 0.15128 %
SOC estimation at end of discharge: 3.6537 %
----------------------------------------------------------------------
Elapsed time is 1.482443 seconds.
----------------------------------------------------------------------
```

Varta battery

```
----------------------------------------------------------------------
Data_07_04_16_03_22 PM_Varta_No3.txt
----------------------------------------------------------------------
Total discharge duration: 4.6205 h
Total energy extracted: 114.1498 Ah
Energy extracted during 1st phase: 44.0535 Ah
Energy extracted during 2nd phase: 70.34 Ah
Depth Of Discharge after 1st phase: 38.5927 %
SOC real after 1st phase: 64.1841 %
SOC estimated after 1st phase: 64.4529 %
SOC estimation error: 0.41869 %
SOC estimation at end of discharge: 5.1923 %
----------------------------------------------------------------------
Elapsed time is 1.825379 seconds.
----------------------------------------------------------------------
```

Banner battery

```
----------------------------------------------------------------------
Data_07_04_16_10_45 AM_Banner_No2.txt
----------------------------------------------------------------------
Total discharge duration: 4.4756 h
Total energy extracted: 117.3729 Ah
Energy extracted during 1st phase: 31.5252 Ah
Energy extracted during 2nd phase: 85.8474 Ah
Depth Of Discharge after 1st phase: 26.859 %
SOC real after 1st phase: 74.1597 %
SOC estimated after 1st phase: 73.9098 %
SOC estimation error: 0.33699 %
SOC estimation at end of discharge: 0.051296 %
----------------------------------------------------------------------
Elapsed time is 1.544104 seconds.
----------------------------------------------------------------------
```

Banner battery

Data_07_05_16_02_20 PM_Banner_No2.txt

Total discharge duration: 3.7323 h
Total energy extracted: 112.0946 Ah
Energy extracted during 1st phase: 0.30092 Ah
Energy extracted during 2nd phase: 111.7929 Ah
Depth Of Discharge after 1st phase: 0.26845 %
SOC real after 1st phase: 99.7533 %
SOC estimated after 1st phase: 99.7488 %
SOC estimation error: 0.0045356 %
SOC estimation at end of discharge: 3.4389 %

Elapsed time is 1.325414 seconds.

Varta battery

Data_07_05_16_09_39 AM_Varta_no4.txt

Total discharge duration: 4.5338 h
Total energy extracted: 119.3932 Ah
Energy extracted during 1st phase: 34.0194 Ah
Energy extracted during 2nd phase: 85.3768 Ah
Depth Of Discharge after 1st phase: 28.4936 %
SOC real after 1st phase: 72.3419 %
SOC estimated after 1st phase: 72.4847 %
SOC estimation error: 0.19729 %
SOC estimation at end of discharge: 0.29633 %

Elapsed time is 1.557905 seconds.

Banner battery

Data_07_08_16_11_51 AM_Banner_no1.txt

Total discharge duration: 4.6659 h
Total energy extracted: 119.8326 Ah
Energy extracted during 1st phase: 40.4973 Ah
Energy extracted during 2nd phase: 79.3729 Ah
Depth Of Discharge after 1st phase: 33.7949 %
SOC real after 1st phase: 66.8055 %
SOC estimated after 1st phase: 66.4613 %
SOC estimation error: 0.5152 %
SOC estimation at end of discharge: -1.9502 %

Elapsed time is 1.726845 seconds.

Banner battery

Data_07_11_16_10_37 AM_Banner_no1.txt

Total discharge duration: 4.3993 h
Total energy extracted: 121.6989 Ah
Energy extracted during 1st phase: 22.4987 Ah
Energy extracted during 2nd phase: 99.1966 Ah
Depth Of Discharge after 1st phase: 18.4872 %
SOC real after 1st phase: 81.5584 %
SOC estimated after 1st phase: 81.3667 %
SOC estimation error: 0.23503 %
SOC estimation at end of discharge: -4.172 %

Elapsed time is 1.871774 seconds.

Banner battery

Data_07_14_16_09_43 AM_Banner_no1.txt

Total discharge duration: 4.039 h
Total energy extracted: 112.0267 Ah
Energy extracted during 1st phase: 21.4621 Ah
Energy extracted during 2nd phase: 90.564 Ah
Depth Of Discharge after 1st phase: 19.158 %
SOC real after 1st phase: 82.4081 %
SOC estimated after 1st phase: 82.2087 %
SOC estimation error: 0.24194 %
SOC estimation at end of discharge: 4.0503 %

Elapsed time is 1.443439 seconds.

Banner battery

Data_07_15_16_05_14 PM.txt

Total discharge duration: 5.2825 h
Total energy extracted: 116.4016 Ah
Energy extracted during 1st phase: 80.0083 Ah
Energy extracted during 2nd phase: 36.5858 Ah
Depth Of Discharge after 1st phase: 68.7347 %
SOC real after 1st phase: 34.4194 %
SOC estimated after 1st phase: 33.7913 %
SOC estimation error: 1.8249 %
SOC estimation at end of discharge: 2.2599 %

Elapsed time is 2.039220 seconds.

Banner battery

Data_07_15_16_11_09 AM_Banner_no1.txt

Total discharge duration: 5.3714 h
Total energy extracted: 119.297 Ah
Energy extracted during 1st phase: 80.0043 Ah
Energy extracted during 2nd phase: 39.3729 Ah
Depth Of Discharge after 1st phase: 67.0631 %
SOC real after 1st phase: 34.4227 %
SOC estimated after 1st phase: 33.7861 %
SOC estimation error: 1.8494 %
SOC estimation at end of discharge: -0.13197 %

Elapsed time is 1.863809 seconds.

Varta battery

Data_07_18_16_03_18 PM_Varta_no3.txt

Total discharge duration: 4.7917 h
Total energy extracted: 116.4367 Ah
Energy extracted during 1st phase: 50.0048 Ah
Energy extracted during 2nd phase: 66.57 Ah
Depth Of Discharge after 1st phase: 42.9459 %
SOC real after 1st phase: 59.3457 %
SOC estimated after 1st phase: 59.6662 %
SOC estimation error: 0.54009 %
SOC estimation at end of discharge: 3.5145 %

Elapsed time is 1.755764 seconds.

Banner battery

Data_07_19_16_01_49 PM_Banner_no2.txt

Total discharge duration: 5.2402 h
Total energy extracted: 114.4531 Ah
Energy extracted during 1st phase: 80.0061 Ah
Energy extracted during 2nd phase: 34.5522 Ah
Depth Of Discharge after 1st phase: 69.903 %
SOC real after 1st phase: 34.4213 %
SOC estimated after 1st phase: 33.7926 %
SOC estimation error: 1.8264 %
SOC estimation at end of discharge: 4.033 %

Elapsed time is 1.851757 seconds.

10.2 **Implementation in Matlab with fmincon**